RIGA TECHNICAL UNIVERSITY

Vivita Priedniece

EXPERIMENTAL STUDY AND MODELLING OF SMALL CAPACITY BOILER FLUE GAS TREATMENT AND HEAT RECOVERY

Summary of the Doctoral Thesis

RTU Press
Riga 2022

RIGA TECHNICAL UNIVERSITY
Faculty of Electrical and Environmental Engineering
Institute of Energy Systems and Environment

Vivita Priedniece
Doctoral Student of the Study Programme "Environmental Science"

EXPERIMENTAL STUDY AND MODELLING OF SMALL CAPACITY BOILER FLUE GAS TREATMENT AND HEAT RECOVERY

Summary of the Doctoral Thesis

Scientific supervisors

Professor Dr. habil. sc. ing.
IVARS VEIDENBERGS

Lead Researcher Dr. sc. ing.
VLADIMIRS KIRSANOVS

RTU Press
Riga 2022

Priedniece V. Experimental Study and Modelling of Small Capacity Boiler Flue Gas Treatment and Heat Recovery. Summary of the Doctoral Thesis. – Riga: RTU Press, 2022. – 48 p.

Published in accordance with the decision of the Promotion Council "RTU P-19" of 14 January 2022, Minutes No. 150.

This work has been supported by the European Social Fund within the Project No. 8.2.2.0/20/I/008 «Strengthening of PhD students and academic personnel of Riga Technical University and BA School of Business and Finance in the strategic fields of specialization» of the Specific Objective 8.2.2 «To Strengthen Academic Staff of Higher Education Institutions in Strategic Specialization Areas» of the Operational Programme «Growth and Employment».

This research was supported by Riga Technical University's Doctoral Grant programme.

This Doctoral Thesis has been developed within the project "Individual Heat Supply with Integrated Fog Unit System (IFUS)" of the European Regional Development Fund, Project No. 1.1.1.1/16/A/015

https://doi.org/10.7250/9789934227608
ISBN 978-9934-22-760-8 (pdf)

DOCTORAL THESIS PROPOSED TO RIGA TECHNICAL UNIVERSITY FOR THE PROMOTION TO THE SCIENTIFIC DEGREE OF DOCTOR OF SCIENCE

To be granted the scientific degree of Doctor of Science, the present Doctoral Thesis has been submitted for the defence at the open meeting of RTU Promotion Council on May 24, 2022 at 14.00 at the Faculty of Electrical and Environmental Engineering of Riga Technical University at Zundas krastmala 8, Room 109.

OFFICIAL REVIEWERS

Professor Dr. sc. ing. Andres Siirde,
Tallin University of Technology, Estonia

Professor Dr. sc. ing. Edmunds Teirumnieks,
Rezekne Academy of Technologies, Latvia

Professor Dr. sc. ing. Gatis Bažbauers,
Riga Technical university

DECLARATION OF ACADEMIC INTEGRITY

I hereby declare that the Doctoral Thesis submitted for the review to Riga Technical University for the promotion to the scientific degree of Doctoral of Science is my own. I confirm that this Doctoral Thesis had not been submitted to any other university for the promotion to a scientific degree.

Vivita Priedniece ……………………………. (signature)
Date: ………………………

The Doctoral Thesis has been written in Latvian. It consists of Introduction, 4 chapters, Conclusions, 38 figures, 17 tables, 67 mathematical formulas; the total number of pages is 105, including annexes. The Bibliography contains 133 titles.

TABLE OF CONTENTS

ABBREVIATIONS

D_2 – calculated droplet diameter, μm;
D_1 – droplet diameter at reference pressure, μm;
P_2 – water pressure used in experiments, bar;
P_1 – reference water pressure, bar;
m_d – droplet mass, kg;
β_p – mass transfer coefficient in case of changes in partial pressure, kmol/(N · s);
dZ – height of the unit element, m;
d_p – particle diameter, m;
d_d – droplet diameter, m;
H – height of the unit, m;
M_v – molar mass of vapour, 18 kg/kmol;
p^{sat} – partial pressure of saturated vapour on the droplet, Pa;
p_b – partial pressure of vapour in the gas flow, Pa;
t_s – saturation temperature of droplets, °C;
p – the total pressure of the system, Pa;
ω – moisture content of gas, kg/kg_{dg};
p_{dg} – partial pressure of dry gas, Pa;
p_{wv} – partial pressure of water vapour, Pa;
u_r – velocity of the water droplet in the unit, m/s;
u_d – droplet velocity, m/s;
u_g – gas velocity, m/s;
u_t – droplet terminal velocity in stationary gas, m/s;
ρ_w – water droplet density, kg/m^3;
ρ_g – wet gas density, kg/m^3;
g – the acceleration of gravity, m/s^2;
C_D – drag coefficient;
μ_g – dynamic viscosity of wet gas, Pa · s;
Stk – the Stokes number of the droplet;
ρ_p – particle density, kg/m^3;
d_p – particle diameter, m;
C_c – the Cunningham correction factor for particle size;
m_g – wet gas mass flow, kg/s;
m_{dg} – dry gas mass flow, kg/s;
m_v – water vapour mass flow, kg/s;
m_w – changes in water mass, kg/s;
V_w – sprayed water flow, m^3/s;
V_g – flue gas flow in the unit, m^3/s;
C_p – particulate matter concentration in flue gas, kg/m^3;
$C_{p\,i}$; $C_{p\,o}$ – particulate matter concentration at the inlet and the outlet of the unit, kg/m^3;
η_d – the number of droplets in the unit at certain time frame, 1/s;
t_g – gas temperature, °C;
T_g – gas temperature, K;
Q_d – heat of the droplet, J/s;
Q_{ht} – heat transfer heat, J/s;
Q_c – vapour condensation heat, J/s;
Q_p – heat of particles, J/s;
V_d – initial volume of the droplet, m^3;
c_{pg} – specific heat capacity of gas, J/(kg · K);
t_d – temperature of water droplets, °C;
c_{pp} – specific heat capacity of particles, J/(kg · K);
α – heat transfer coefficient from gas to droplet, W/m^2 · K;
β_c – mass transfer coefficient, m/s;
Nu – the Nusselt number;
Sh – the Sherwood number;
λ_g – thermal conductivity coefficient of gas, W/(m · K);
D_v – diffusion coefficient of vapour, m^2/s;
μ_g – dynamic viscosity of gas, kg/(m · s);
ν_g – kinematic viscosity of gas, m^2/s;
$\frac{dt_g}{dZ}$ – change in flue gas temperature, °C;
n_{sk} – the number of droplets in the unit, 1/s;
$\frac{dt_w}{dZ}$ – change in water temperature, °C;
$\frac{dd_d}{dZ}$ – change in water droplet diameter, m;
$\frac{du_d}{dZ}$ – change in droplet velocity, m/s;
$\frac{dC_p}{dZ}$ – change in particulate matter concentration, kg/m^3;

$\frac{d\omega}{dZ}$ – change in gas moisture content, kg/kg_{da};
t_{w1}; t_{w2} – sprayed water temperature before and after the fog unit accordingly, °C;
G – sprayed water amount or flowrate, l/h;
O_2 – oxygen concentration in flue gas, %;
η_{fu} – the efficiency of the fog unit, %;
Q_{con} – the amount of fuel energy consumed in the system, kWh;
ΔQ – the difference between experimental and calculated capacities of the fog unit, %;
$Q_{exp.}$ – the capacity of the fog unit in experiments, kW;
$Q_{calc.}$ – the capacity of the fog unit in calculations, kW;
Q – the capacity of the fog unit, kW;
b_0 – intercept;
b_i; b_j; b_{uj}; b_{jj} – coefficients of variable parameters;
ϵ – error;
Z_n – the nth independent variable;
Z_n^0 – point with coordinates up to k;
ΔZ_n – interval of variables for Z_n axis;
x_n – variable in non-dimensional coordinates;
b_n – the nth coefficient;
N – the number of experiments;
x_{ni} – the variable of each experiment at corresponding b coefficient;
y_i – the dependent variable at corresponding x;
γ – the proportionality coefficient in optimization;
$\delta' k$ – the change step of the parameter in optimization.

INTRODUCTION

Topicality of the Doctoral Thesis

In 2009 the European Commission renewed the Ecodesign Directive (2009/125/EC), which states that all energy generating and consuming equipment, including combustion equipment used for providing heat and hot water, must implement greenhouse gas reducing technologies.

The Ecodesign Directive has set out desirable energy efficiency and created emission amount of combustion equipment. In addition, the World Health Organization has set daily and annual emission value limits, which, when exceeded, cause a significant impact to human health. Individual countries have also included different emission value limits in normatives that industry and individual emission generators must abide by. International and local scale legislation also includes limits for specific emission levels. All the documents have a focus on gaseous pollutants such as carbon dioxide, nitrogen oxides, sulphur oxides, carbon monoxide, and a large part also includes or will include limits for particulate matter emissions.

Particulate matter emissions are an increasing problem at a global scale not only due to generated pollution, but also because studies show a link between increase in respiratory and cardiovascular diseases in case of long-term exposure to particulate matter. The main source of particulate matter is the household sector where small capacity solid biofuel combustion equipment is mostly used.

Flue gas treatment after small capacity combustion equipment is little studied. Technologies developed now are not economically feasible or have low efficiency. Modelling of heat and mass transfer processes is little studied, more detailed studies have been carried out for operation of the equipment in the system, but not for the modelling of particulate matter capture.

Flue gas treatment unit, which additionally provides heat recovery from flue gas and is suitable for use after small capacity boilers that are mostly used in households, has been developed and experimentally tested within the framework of the Doctoral Thesis. The use of this kind of device significantly reduces pollution created by the household sector. In addition, a heat and mass transfer model has been developed with an accompanying differential equations system for the calculations of changes in the main parameters. Treatment process modelling has been done in the model, which offers an opportunity to predict and theoretically determine efficiency of the unit at specific operation parameters of the system, potentially increasing the possibilities of use of the unit with different boilers and fuel types.

The aim and tasks of the Doctoral Thesis

The aim of the Doctoral Thesis is the development, experimental and analytical study and optimisation of operational regimes of the unit meant for small capacity heat source flue gas treatment and heat recovery.

The tasks for fulfilling the aim:

- To calculate and develop the small droplet flue gas condenser, also called the fog unit (FU), and perform experimental study of it.
- To develop a simulation model of the unit and establish the calculation computer programme for it.
- To validate the FU model.
- To perform optimisation of the FU operational regimes using the Box-Wilson method.

Hypothesis

Is it possible to develop an effective particulate matter capture and flue gas heat recovery equipment for household heat sources?

Scientific significance

A new type of condenser technology for small capacity boilers in households for the removal of particulate matter from wet flue gas – the fog unit – is described in the Thesis. Flue gas treatment and latent heat recovery from flue gas occurs in the fog unit simultaneously. The flue gas cooling and treatment is achieved by using small water droplets with diameters below 800 µm. To analyse the unit, a calculation model describing heat and mass transfer was developed using the open access programming language *Python*. This is the first calculation model that describes parameter changes inside the condenser – at the height of the unit, if the particulate matter participates in heat and mass transfer processes. The model was verified at boiler capacities of 10 kW and 20 kW using wood pellets as fuel.

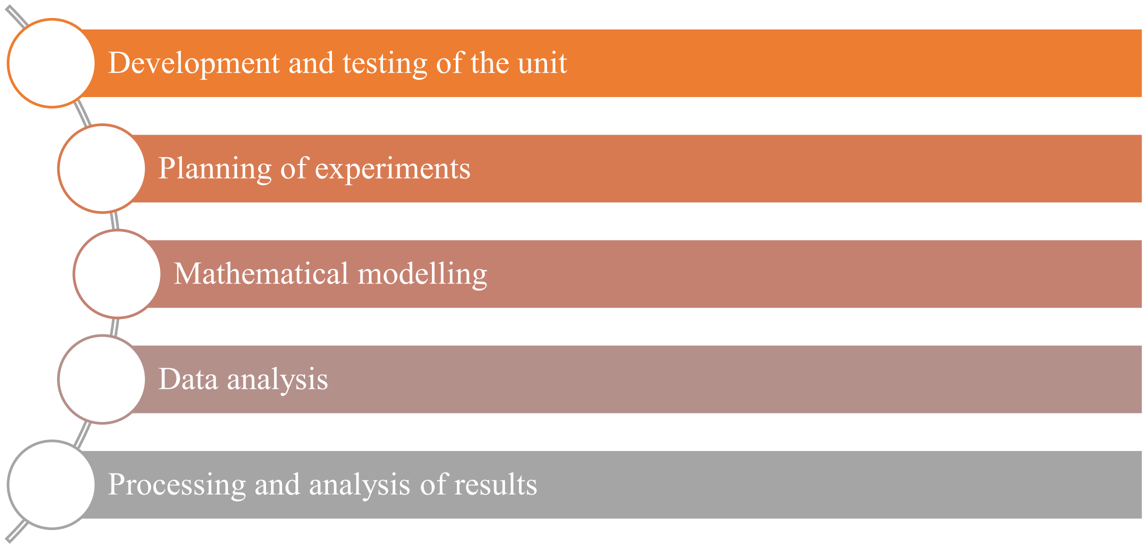

Fig. 1. Implementation algorithm of the Doctoral Thesis

The main stage of the work on the Thesis was the development and testing of the unit, including the primary experiments for verifying the components of the system. After this stage, the most suitable nozzle, sprayed water flowrate and temperature, was determined. Then followed planning and performing of experiments for verifying the fog unit at different operational parameters, development of the mathematical model for describing the operation of the unit, and the analysis of experimental and calculated data. The stage of processing and analysis of results also includes the validation of the model and determination of optimal parameters for using the fog unit in the wood pellet boiler system.

Practical significance

A new type of condenser technology for particulate matter capture from wet flue gas is developed and experimentally tested within the framework of the Thesis. A calculation model was developed for the analysis of the unit operation, which includes a system of differential equations for analysis of the main system parameters – calculations of changes in sprayed water droplet diameter, velocity, flue gas temperature, sprayed water temperature, particulate matter concentration, and gas moisture content. The model was validated using experimental data and has a high confidence level with difference between the results below 10 %. The analysis of the unit was performed at different boiler capacities, offering the most suitable operational regimes to achieve the highest efficiency at real conditions.

The results obtained in the Thesis can be used by decision makers and legislation developers to ensure the increase of the use of flue gas treatment equipment and to establish the requirements for their implementation, especially in households. Industry can use the obtained knowledge and results for the production of the fog unit and similar equipment. At the municipal and country level, there is an opportunity to enhance air quality control by promoting and providing support for inhabitants for the implementation of flue gas treatment equipment.

Approbation of the research

The results of the Doctoral Thesis have been presented at five conferences, in nine scientific publications and one monograph. The research results have been discussed and presented at the following **conferences**:

1. Blumberga, D., Priedniece, V., Veidenbergs, I. Mathematical model of the fog unit. International Scientific Conference of Environmental and Climate Technologies (CONECT 2018), Latvia.
2. Priedniece, V., Kirsanovs, V., Dzikēvičs, M., Vīgants, Ģ., Veidenbergs, I., Blumberga, D. Laboratory Research of the Flue Gas Condenser – Fog Unit. 10th International Conference on Applied Energy (ICAE2018), 22–25 August 2018, Hong Kong, China.
3. Priedniece, V., Kalniņš, E., Kirsanovs, V., Dzikēvičs M., Veidenbergs, I., Blumberga, D. Sprayed water flowrate, temperature and drop size effects on small capacity flue gas condenser's performance. International Scientific Conference of Environmental and Climate Technologies (CONECT 2019), Latvia.
4. Priedniece, V., Kalnins, E., Kirsanovs, V., Pedisius N., Vīgants, Ģ., Veidenbergs, I., Blumberga, D. Particulate Matter Emission Decrease Possibility from Household Sector using Flue Gas Condenser – Fog Unit. Analysis and Interpretation of Results., International Scientific Conference of Environmental and Climate Technologies (CONECT 2019), Latvia.
5. Priedniece, V., Kirsanovs, V., Prodaņuks T., Veidenbergs, I., Blumberga, D. Treatment of particulate matter pollution: people's attitude and readiness to act. International Scientific Conference of Environmental and Climate Technologies (CONECT 2020), Latvia, Zoom platform.

Scientific publications and monograph

1. Seļivanovs, J., Vīgants, E., Priedniece, V., Veidenbergs, I., Blumberga, D. Flue Gas Treatment Multi-Criteria Analysis. Energy Procedia, Elsevier, 2017, pp. 379–385. ISSN 1876-6102. Available: doi:10.1016/j.egypro.2017.09.056.
2. Priedniece, V., Kirsanovs, V., Dzikēvičs, M., Vīgants, Ģ., Veidenbergs, I., Blumberga, D. Laboratory Research of the Flue Gas Condenser – Fog Unit. *Energy Procedia*, 2018, Vol. 147, pp. 482–487. ISSN 1876-6102. Available: doi:10.1016/j.egypro.2018.07.056.
3. Priedniece, V., Kirsanovs, V., Dzikēvičs, M., Vīgants, Ģ., Veidenbergs, I., Blumberga, D. Experimental and Analytical Study of the Flue Gas Condenser – Fog Unit. *Energy Procedia*, 2019, Vol. 158, pp. 822–827. ISSN 1876-6102. Available: doi:10.1016/j.egypro.2019.01.215.
4. Priedniece, V., Kalnins, E., Kirsanovs, V., Pedisius N., Vīgants, Ģ., Veidenbergs, I., Blumberga, D. Particulate Matter Emission Decrease Possibility from Household Sector using Flue Gas Condenser – Fog Unit. Analysis and Interpretation of Results. *Environmental and Climate Technologies,* 2019, Vol. 23, Issue 1, pp. 135–151. ISSN 2255-8837. Available: doi.org/10.2478/rtuect-2019-0010.
5. Priedniece, V., Kalniņš, E., Kirsanovs, V., Dzikēvičs M., Veidenbergs, I., Blumberga, D. Sprayed water flowrate, temperature and drop size effects on small capacity flue gas condenser's performance. Environmental and Climate Technologies, 2019, Vol. 23: Issue 3, pp. 333–346. Available: https://doi.org/10.2478/rtuect-2019-0099.
6. Blumberga, D., Priedniece, V., Rumba, R., Kirsanovs, V., Ņikitenko, A., Lavendelis, E., Veidenbergs, I. Mathematical Modeling of Heat and Mass Processes in a Scrubber: The Box–Wilson Optimization Method. Energies, 2020, Volume 13, Issue 9, Available: https://doi.org/10.3390/en13092170.
7. Kirsanovs, V., Priedniece, V., Kalniņš, E., Veidenbergs, I., Blumberga, D. Innovative Scrubber Technology Model for Domestic Boiler Application, International Journal of Energy and Environmental Engineering, 2020, Available: https://doi-org.resursi.rtu.lv/10.1007/s40095-020-00347-z.
8. Kirsanovs, V., Priedniece, V., Kalniņš, E., Veidenbergs, I., Blumberga, D. Small Scale Pellet Boiler Gas Treatment in Fog Unit. International Journal of Energy and Environmental Engineering, 2020, Available: https://doi-org.resursi.rtu.lv/10.1007/s40095-020-00357-x.
9. Priedniece, V., Kirsanovs, V., Prodaņuks T., Veidenbergs, I., Blumberga, D. Treatment of particulate matter pollution: people's attitude and readiness to act, Environmental and Climate Technologies, 2020, 24(2), pp. 231–246. Available: https://doi.org/10.2478/rtuect-2020-0069.

- Barisa, A., Blumberga, A., Blumberga, D., Grāvelsiņš, A., Gušča, J., Lauka, D., Kārkliņa, I., Muižniece, I., Pakere, I., Priedniece, V., Romagnoli, F., Rošā, M., Seļivanovs, J., Soloha, R., Veidenbergs, I., Vīgants, E., Vīgants, Ģ., Ziemele, J. Energosistēmu analīze un modelēšana. Rīga: RTU Izdevniecība, 2018. 144 lpp. ISBN 978-9934-22-037-1.

1. SUMMARY OF THE LITERATURE REVIEW

Households are an insufficiently studied particulate matter (PM) pollution source, with practically no control by legislation. There are no developed economically feasible and effective technologies for small capacity boiler flue gas treatment. One legislation document that includes emission reduction measures for small capacity combustion equipment is the Directive 2009/125/EC of the European Parliament and of the Council with whom it is possible to provide development of the system to determine ecodesign requirements for energy related products [1] and related regulations of the Cabinet of Ministers (CM) of the Republic of Latvia (LR) No. 941 "Regulations for ecodesign requirements for energy related products" [2]. Regulations of the Ecodesign Directive for households state that the following:

- for boilers with automatic fuel feed, PM emissions in the heating season must not exceed 40 mg/m^3, and for boilers with manual fuel feed– 60 mg/m^3;
- seasonal space heating efficiency for boilers with capacity up to 20 kW (including) must not be below 75 %;
- seasonal space heating efficiency for boilers with capacity above 20 kW must not be below 77 % [1].

Emissions reduction technologies for products from combustion processes are divided into primary and secondary technologies. Primary technologies focus on fuel quality, furnace and boiler design, but secondary technologies focus on flue gas treatment and processing [3]. The technologies developed for emissions reduction from small capacity boilers are:

- additives for fuel,for example, calcium hydroxide ($Ca(OH)_2$), limestone ($CaCO_3$) and kaolin ($Al_2Si_2O_5(OH)_4$) [4];
- catalytic filters (for example, with platinum, palladium coating) [5];
- small capacity electrostatic precipitators (not economically feasible) [6];
- small pipe heat exchangers [7];
- PM filters (can increase emissions of smaller particles) [4].

All flue gas treatment technologies have a single disadvantage – residues from the treatment process. In case of dry methods those are solid residues, but in case of wet treatment methods – liquids with solid residue additions. It is necessary to evaluate the use of these residues further. It must be noted that neither of the most widely used flue gas treatment methods is suitable for small capacity boilers in households due to high or additional expenses that are related with residue treatment and operation.

In treatment of hot contaminated gases from PM, in direct contact units, particulate capture by water droplets occurs simultaneously with heat and mass transfer on the surface of droplets and wet contaminated gases. Characteristic parameter changes inside the condenser during flue gas cooling and treatment process have been little studied. It is useful to use the heat recovered by water for household needs. This increases the energy efficiency not only of the unit, but also of the total heating and hot water preparation system. PM impact on heat and mass transfer processes is little studied. In modelling processes, the total heat and mass transfer in the flow is mainly studied, as well as removal of gaseous pollutants from flue gas.

PM is divided into coarse (2.5–10 μm), fine (< 2.5 μm) and submicron (< 0.1 μm) particles. Milling and cutting processes are the main sources of coarse PM and when inhaled they enter the respiratory tract. Fine particles occur in combustion processes. These particles make up to 50 % of all PM in air and they remain there for a long time – weeks, even months [8]. Fine particles can get deeper in the respiratory tract – lungs and even into the blood stream.

PM is a significant pollution problem because the limits set for PM concentrations in air given in the EU Directive 2008/50/EC on air quality and cleaner air in Europe are regularly exceeded [9], [10]. The EU strategies on emissions reduction do not directly include PM emissions, but they include gaseous emissions, which can increase the impact of pollution and can cause secondary PM [6]. Over 45 % of PM emissions in Europe in 2015 were caused by small capacity combustion equipment. Performed studies have proven that the biomass use in combustion equipment can make up 19–37 % from the total created PM amount, depending on climate conditions and seasonality, as well as on the used fuel type [11], [12].

PM pollution is a topical problem on a global scale. The World Health Organization (WHO) has developed guidelines for created PM emissions, which is based on data evaluation from the studies performed by experts, and it is applicable to any country. PM emissions have set limit values for $PM_{2.5}$ and PM_{10} particles. The average annual limit value for $PM_{2.5}$ concentration is 10 $\mu g/m^3$, but for PM_{10} it is 20 $\mu g/m^3$. The average daily emissions concentrations for $PM_{2.5}$ is up to 25 $\mu g/m^3$, but for PM_{10} – 50 $\mu g/m^3$ [13].

The model described in the Thesis was developed using programming language *Python*, which is an open access, platform independent, object-oriented, and universal programming language that is faster and gives out higher quality results when compared with *Java* or *C* programming languages. It has gained popularity in the recent years due to wide use and in-depth syntax. The program provides a more compact depiction of the problem, therefore reducing model development time and maintenance expenses. A wide base library and several thousands of additional libraries provide program developers with high quality solutions that can be easily included in existing systems to achieve almost any goal [14].

The example of *Python* use is a developed defect analysis tool (*PyCDT*) to perform defect calculations with widely used density functional theory programmes. The tool gives an access to a database of materials that allows analysis of possible point type defects for different materials [15]. *SAMT2* is an improved spatial analysis and modelling tool in a form of a *Python* module. The tool is widely used – easily adjustable and improved, without changes in used data types [16]. Another example of *Python* use is as an uncertainty analysis tool in environmental modelling. The model is based on the Bayes linear theory also known as linear first order second-moment uncertainty analysis, with an improved user side. The aim of the model is to improve resource management with additional uncertainty analysis. It can be adjusted to different environmental systems if text files are used for model operation and results can be read from the files without additional processing. The calculations are re-written in the program code. In case of iterative process study where the closest observation is searched, calculations are repeated thousands of times that extends the determination time up to an hour or more [17]. In the case of the model developed in the Thesis, the use of text files and iterative calculations process is also significant.

2. EXPERIMENTS FOR ANALYSIS OF THE FOG UNIT OPERATION

2.1. The fog unit experimental stand

The fog unit (FU) experimental stand is made of five parts: solid fuel boiler, the FU reactor, ducts for flue gas input and outlet with connections for measuring devices, hydraulic system, and pulp tank (see Fig. 2.1).

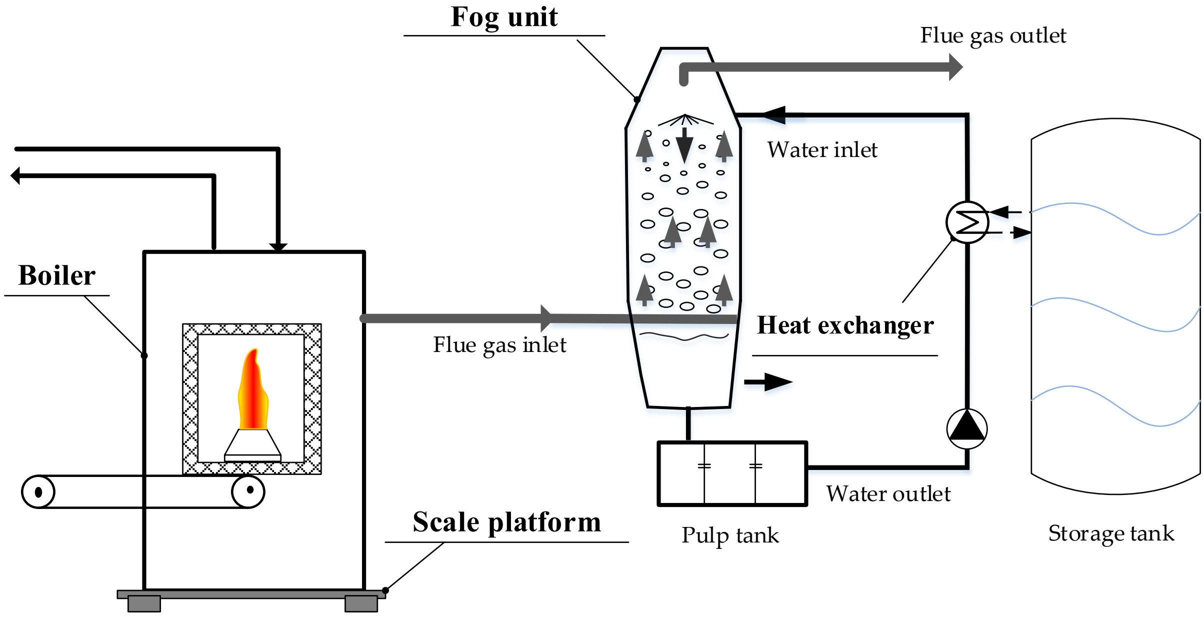

Fig. 2.1. Scheme of the fog unit experimental stand

Making of the experimental stand included the testing of separate stand components in the laboratory environment. A pellet boiler *Grandeg Bio-25* is used in the system, which provided the necessary capacity, generated heat, and flue gas amount. The boiler is connected with the FU using flue gas duct that has several measuring device sensors – for flue gas analyser *Testo 350*, hygrometer, temperature sensors and differential pressure measurement device. Additionally, flue gas pipe has a connection for inserting the PM measuring probe.

The FU is mounted behind the boiler and consists of casing (see Fig. 2.2), spraying nozzle, flue gas inlet and outlet, pulp tank and water inlet pipe and separator. The flue gas inlet is located at the lower part of the unit where boiler flue gas duct is connected. Flue gases, entering the unit, move to the upper part of the FU where flue gas outlet and water inlet pipes are located. The nozzle that provides water spraying in the unit is mounted on the end of the water inlet pipe. The whole casing of the unit is covered with heat insulation material to reduce heat losses from the unit in the surrounding environment. The operation of the unit is based on a small droplet or fog zone created by water spraying, where the sprayed water mixes with counter flowing flue gases. Direct contact heat and mass transfer occurs between flue gas and water, PM is captured with the help of droplets, which are then discharged to the pulp tank.

The flue gas duct is located behind the FU, to outlet the cleaned flue gases to the chimney and afterwards in the surrounding environment. In the flue gas duct right after the FU, metal shavings are inserted, to delay water droplet movement and settling in the flue gas ducts outside the FU. There, connections for temperature sensors, hygrometer, and differential pressure measurement device, as well as for probe of PM measuring device, are located. In the upper part of the flue gas duct, after the FU chimney, a smoke exhauster is mounted to provide the necessary traction for flue gas movement through the unit.

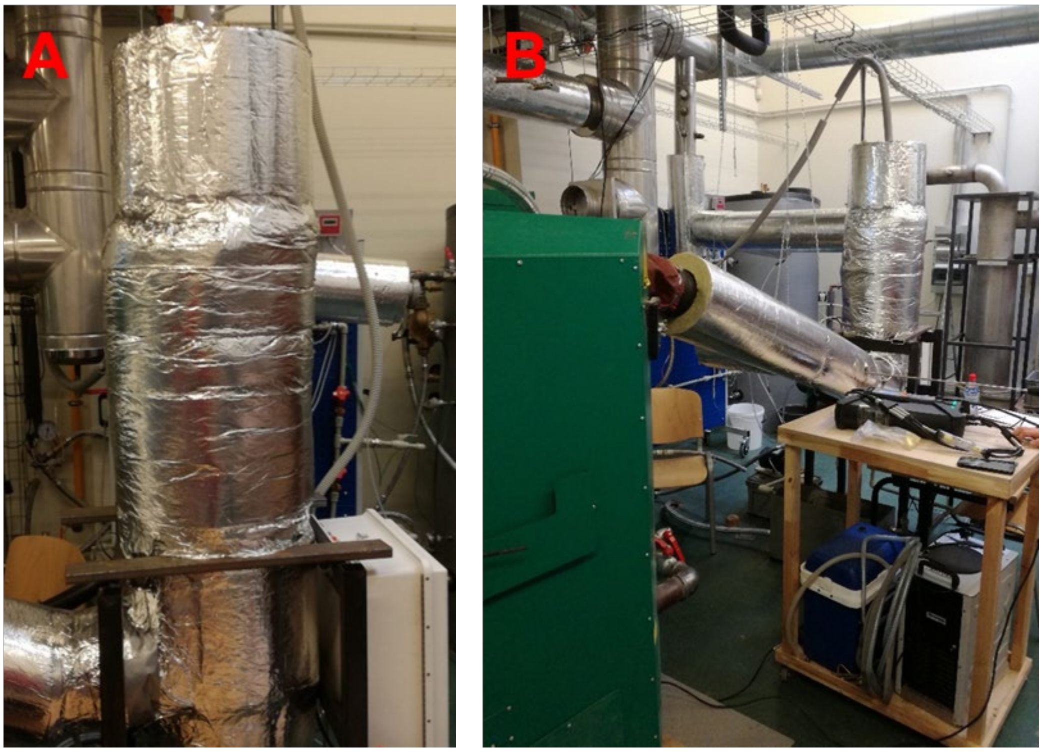

Fig. 2.2. The fog unit in the experimental stand:
A – the fog unit up-close; B – the fog unit from the boiler side

The hydraulic system consists of water supply pipes, fastenings, and transitions. The pipes have connections for manometers, water flow meters, deaerator, and temperature sensors. With the help of hydraulic system and nozzle, water is let into the FU, then from the FU, water with captured PM moves to the pulp tank. The circulation pump provides water movement from the fog unit to the heat exchanger, where heat is recovered from the water that goes through the FU, to ensure that the sprayed water temperature remains equal. The recovered heat is accumulated in the storage tank, with a volume of 500 l. The circulation pump is equipped with a frequency convertor for water flowrate regulation. After the heat exchanger water is moved back to the FU.

The pulp tank for water treatment consists of a small metal box, which, with the help of metal plates, is divided into three parts. Each of the metal plates have a drilled hole in the middle to provide water flow from one side of the tank to the other. Further, with the help of circulation pump, water is moved back to the FU. The largest part of PM settles in the first part of the tank and the smallest part – in the last part of the tank. Simultaneously to the FU development, the development and improvement of new pulp treatment equipment is carried out. The initial pulp tank solution is replaced by a compact PM collector. It is a new and effective technology that provides the PM separation from water to ensure that water can be returned to the FU system without creating additional risks. The operation principle and prototype of the new device is based on a radial sedimentation tank. The development and testing of the PM pulp treatment device is described in the studies of Švedovs, et al., therefore, this component is not studied in detail within the framework of the Thesis [18], [19].

Verification of moisture measurement devices was carried out at 32 %; 75 %; and 94 % relative humidity (RH), using the climate chamber and dissolved salt method. The salts used in these tests were MgCl (32 % RH); NCl (75 % RH), and KNO_3 (94 % RH). The largest absolute deviation was observed for one of the sensors, which was 0.6 % RH, or relatively 2.5 %. Deviation values were used to develop an equation for correction coefficient calculations. The equation is input in the data logger, saving the original data, and simultaneously calculating the corrected value.

Flue gas analyser *Testo 350* was calibrated in laboratory conditions. It gets connected with special gas cylinders, which are filled with O_2, CO_2, CO, and NO gas mixture. Gases in cylinders have a known concentration, therefore they are suitable for performing calibration. Calibration was performed at least once a month or after every 10 tests.

The description, choice and testing of nozzles (see Fig. 2.3) were performed and described at a separate study [20]. The main characteristic parameters for a nozzle are spraying pressure and angle, sprayed water velocity, spraying height, and spraying cone. These parameters, in turn, are affecting the surface made by the nozzle and water droplet diameter [20].

Fig. 2.3. Nozzle testing [20]

Full cone nozzles were chosen for the FU system, which creates a full water droplet flow, their spraying angle at a 3-bar water pressure has to be 90°, and it has to provide a sprayed water flowrate of approximately 3.7 l/min at a pressure of 2 bars. The nozzle spraying height in the FU is constant, therefore, it was not changed during the nozzle testing. Equal sprayed water flowrate was used to determine how spraying angle changes depending on the nozzle size. The narrowest spraying angles were obtained with the largest nozzle, and the widest angles were obtained with the smallest nozzle [20].

It was determined that the sprayed water cone formed by the nozzle is not homogenous. The amount of sprayed water at some points was 2–3 times bigger than at other points. The droplet size and velocity was determined using photo fixation. The spraying process was recorded using 100 frames per second, and light impulses with a length of 1/20 000 per second were used to obtain the pictures of fixed droplets. The water droplet size was determined in metric units by fixating a reference scale [20].

Particulate matter measurement procedure

PM measurement procedure is a very careful process performed with high precision. Obtained results are significant to determine the PM capture efficiency of the unit. The PM measurement process can be divided into five stages: filter selection, dish preparation, filter preparation, filter use in experiments and filter analysis. The filters were selected based on the requirements of Standard *LVS EN ISO:9096* [21], based on which the experiments were carried out. The PM measurement device also complies with the mentioned standard. The filters used in experiments are of round shape and made from glass fibre or quartz.

Before starting PM measurements, the filter is placed in the nozzle of the probe. Before each test, a leak check of the device is performed. Duct related parameters are input in the data panel of the device – depth of the measurement point and radius, duct shape, flue gas parameters (oxygen and CO_2 concentration in the duct), as well as the duration of the test. The test is started after the data input. PM measurements are performed according to the requirements given in Standard *LVS EN ISO 9096:2017*. The method used in PM measurements before and after the FU is manual PM concentration determination in standard conditions from stationary emissions source. The sampling occurs using inner filtration method in isokinetic conditions. In isokinetic sampling, input gas velocity and direction in the sampling probe is the same as in the duct at the specific sampling point.

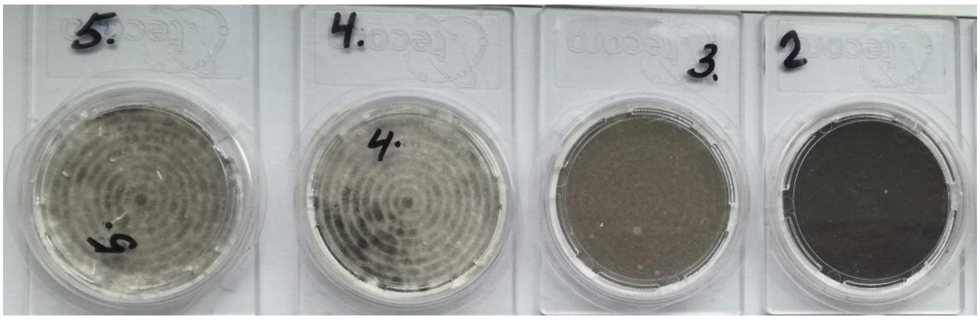

Fig. 2.4. Filters with different particulate matter concentrations

Mass difference is determined using the initial and final mass of the filter. Using the PM measuring device, the initial injected flue gas volume was determined, which is then referred to weighted PM amount, obtaining the resulting PM concentration. PM concentration on filters is different as seen in Fig. 2.4. The lighter colour filters are with lower PM concentration, and they were used in measurements at smaller sprayed water flowrates in the unit. Filters are numbered, accordingly from left to right – 5, 4, 3 and 2. Filter No. 5 was used for PM measurements after the FU at sprayed water flowrate 200 l/h, Filter No. 4 was used for PM measurements after the FU at sprayed water flowrate 150 l/h, Filter No. 3 was used for PM measurements after the FU at sprayed water flowrate 50 l/h, however, Filter No. 2. was used to determine PM concentration before the FU, after the boiler, without spraying. Similar situation was observed for all used nozzles.

2.2. Implementation of experiments

For implementation of experiments, five variable parameters were defined that describe flue gas and water sprayed into the unit: sprayed water temperature, sprayed water flowrate, sprayed water droplet diameter, flue gas flow, and flue gas temperature at the inlet of the unit.

Sprayed water temperature t_{w1} determines, how much heat is obtained from flue gas flowing through the FU. Three different sprayed water temperatures were used in experiments, rounded to 20 °C, 30 °C, and 40 °C, accordingly. Another important variable factor that affects the absolute moisture content, recovered heat, PM capture and flue gas temperature, is **sprayed water amount or flowrate G** through the FU. Sprayed water flowrates used in initial experiments were in a range from approximately 50 l/h to 250 l/h, with a change of 50 l/h. **Initial diameter of sprayed water droplets d_{d0}** is another water describing parameter that is directly related to nozzle and its size. Three different sized *MaxiPass L* (*MPL nozzle number*) nozzles were used in experiments – *MPL 0.77*, *MPL 1.12* and *MPL 1.51* (see Fig. 2.5). These nozzles are durable against clogging, and they can be used with water having a small particulate matter addition, which is a significant advantage.

The main parameters related with flue gases, which can be controlled during experiments, are flue gas flow and flue gas temperature at the inlet of the unit. Both parameters are dependent on boiler parameters – capacity, efficiency, operational regime. **Flue gas flows (V_g)** tested in initial experiments are in a range from 0.0194 Nm^3/s to 0.0226 Nm^3/s, whereas **flue gas temperature (t_{g1})** after the boiler and before the FU is in a range from 130.8 °C to 135.2 °C. These parameters change minimally because testing of the system was performed at constant boiler parameters.

Fig. 2.5. Nozzles used in experiments

Droplet diameters were calculated at different flowrates and nozzles. Results of several tests were used in calculations. Droplet diameter at each flowrate and nozzle size was calculated four times to obtain a more precise average value. The obtained droplet diameters were calculated using an equation given by nozzle producers:

$$D_2 = D_1 \times \left(\frac{P_2}{P_1}\right)^{-0.3} \quad (2.1)$$

Table 2.1

The Calculated Droplet Diameters at Different Nozzles and Water Flowrates

		Flowrate, l/h			
		50	150	200	250
Nozzle *MPL 0.77*	Droplet diameter, μm	307	192	161	-
		315	198	166	
		316	198	166	
		320	200	168	
	Average value	314	197	165	
Nozzle *MPL 1.12*	Droplet diameter, μm	451	270	-	200
		453	272		201
		478	287		212
		450	270		200
	Average value	458	275		203
Nozzle *MPL 1.51*	Droplet diameter, μm	794	398	-	275
		786	394		272
		786	394		273
		785	393		272
	Average value	788	395		273

The largest droplet diameters were obtained at the flowrate of 50 l/h, up to 794 μm. The smallest droplet diameters were obtained at the flowrate of 250 l/h, up to 192 μm. There were significant differences in droplet diameters that were observed depending on the nozzle used. For example, droplet diameter for nozzle *MPL 1.51* at water flowrate 50 l/h on average was 788 μm, but for nozzle *MPL 0.77* – 314 μm.

3. CALCULATION MODEL FOR THE FOG UNIT OPERATION ANALYSIS

3.1. Droplet movement in wet gas flow in condensation

The FU is designed for wet gas treatment using water spraying. When water droplets interact with gas flow and PM, vapour condensation and PM capture occurs. Processes between wet gases and dispersed water droplets are observed in direct contact condensers [22].

Droplets collide during movement and, as a result, they either coalescence or divide into smaller droplets. Coalescence efficiency is high, and it can be observed in most cases of collision. As a result, the division of droplet diameters becomes polydisperse. Droplet collision efficiency is inversely proportional to the droplet diameter. Larger sized droplets push off very small droplets because a layer of compressed gas is formed under the large sized droplet [23]. The assumptions in the model development are as follows:

- the distribution of droplets and PM is homogenous with determined initial diameters, accordingly d_{d0} and d_p;
- the volume and surface temperature of droplets are equal, due to small droplet sizes;
- PM velocity and temperature are equal to gas velocity and temperature;
- radiation heat is not considered in heat transfer because process temperatures are low;
- it is assumed that coalescence and division of droplets, due to collision, are the same;
- dry gas flow in the unit is constant;
- droplets are spherical;
- the Archimedes' principle is not taken into account in droplet movement;
- gas flow changes resulting from PM capture are neglected;
- PM capture occurs due to inertia mechanism;
- gas is considered as an ideal gas to which the gas state equation applies.

Droplet movement and wet gas flow in the unit are counter flows. The droplet mass changes in the process, and it increases in the case of condensation. Heat and mass transfer processes occur during the time that droplets spend in the FU. As direction of the Z axis is opposite to the direction of droplet movement, the mass changes, if the driving force is the difference between vapour partial pressures, can be expressed as

$$\frac{dm_d}{dZ} = -\beta \frac{\pi d_d^2}{H} M_v (p_b - p^{sat}), \ \mathrm{kg}/(\mathrm{m \cdot s}) \quad (3.1)$$

For determination of saturated vapour partial pressure, the following equation is used [24]:

$$p^{sat} = 610.78 \exp\left(\frac{17.27 \times t_s}{t_s + 237{,}3}\right) \quad (3.2)$$

Partial pressure of vapour in gas flow is determined using the gas moisture content:

$$p_b(t_b) = \frac{p\omega}{0.622 + \omega} \quad (3.3)$$

The total pressure of wet gas is a sum of components' partial pressures:

$$p = p_{dg} + p_{vb} \quad (3.4)$$

In equipment without increased pressure, the total pressure is assumed as p = 101 325 Pa.

Several velocities were determined for vertical droplet movement in gas flow: terminal velocity of the droplet, flow velocity, and droplet velocity in the unit. The real droplet velocity in flow determines the time that a droplet spends in the unit. Velocity is a vectorial quantity described by value and direction. To determine the velocity of a water droplet in the unit u_r, it is necessary to consider the forces impacting the droplet: the gravitational force, the opposite Archimedes' force and the force of the frontal resistance of the droplet. The droplet will move with velocity u_r if there is a balance between the forces. Terminal velocity for a spherical droplet in stationary gas is determined with the following equation:

$$u_t = \sqrt{\frac{4(\rho_w - \rho_g) g d_d}{3 \rho_g C_D}}, \text{m/s} \quad (3.5)$$

The relationship between terminal and relative droplet, the droplet and gas velocities is determined as in [25]:

$$u_t = u_r = u_d + u_g, \text{m/s} \quad (3.6)$$

As the drag coefficient is dependent on the droplet movement regime, then a *Re* number describing movement regime has to be known, which includes u_r to determine it:

$$Re = \frac{u_r d_d \rho_g}{\mu_g} \quad (3.7)$$

The relationship between the terminal velocity and drag coefficient is determined by a balance of gravitational and resistance forces. Calculations are complicated by the fact that C_D is not constant, and for different movement regimes the drag coefficient changes are determined by different laws: Stokes, Oseen, and Goldstein laws. Each law applies to a small *Re* change range. By increasing the *Re* change range, empirical or partially empirical drag coefficient calculation equations are used in practice [26]. The authors in [27] offer a unified relationship for the Re change range $0.1 \leq Re \leq 3 \cdot 10^5$, which is shown further:

$$C_D = \frac{24}{Re}(1 + 0.197 Re^{0.63} + 2.6 \times 10^{-4} Re^{1.38}) \quad (3.8)$$

Gradual approximation or iteration methods are used in calculations. The *Re* value is assumed and the drag coefficient is calculated using Equation (3.8). The relative droplet velocity is calculated with Equation (3.6) and the *Re* value is recalculated using Equation (3.7). Calculations are repeated until the calculated value matches with the assumed value. The u_r and *Re* values determined during the iteration process have to be used in the following calculations.

Two forces leave an impact on a particle, which moves in the gas flow – gravitational force and the opposite friction force. The Archimedes' force in gas is small and it can be neglected. The droplet velocity in gas flow can be expressed with an equation:

$$\frac{du_d}{dZ} = \frac{3 C_D u_r \mu_g Re}{4 \rho_w d_d^2 u_d} - \frac{g}{u_d}, \text{m/(m} \cdot \text{s)} \quad (3.9)$$

Changes in droplet diameter are related to droplet mass changes due to the water vapour condensation. In this case, the droplet diameter changes related to droplet collision are not considered. Droplet diameter changes are determined using the equation below:

$$\frac{dd_d}{dZ} = -\frac{2\beta_p M_v(p_b - p^{sat})}{\rho_w u_d}, \text{m/m} \tag{3.10}$$

It should be noted, that the equation determines diameter changes in a specific range – an element. To determine the value of a diameter at the output of an element, a value at the input of an element has to be added to the increase in diameter. An initial droplet diameter d_{d0} is assumed or calculated if a distribution law after the nozzle is known for droplets diameter [28].

3.2. Particulate matter capture by a droplet

As the droplet moves through contaminated gas flow, it captures PM and cleans gas. It is assumed that particles and gas move with the same velocity and there is no relative movement of PM and gas. Wet scrubbers have inertial impaction, interception and diffusion PM capture mechanisms [29]. Diffusional phoresis, thermophoresis, electric field and other mechanisms can operate in specific cases [30]. Inertial impaction is the leading mechanism in PM capture from fuel combustion producst in spraying scrubbers [31]. The PM capture efficiency of a droplet in case of inertial impaction mechanism can be calculated as in [32]:

$$\eta_d = \left(\frac{Stk}{Stk + 0.35}\right)^2 \tag{3.11}$$

$$Stk = \frac{d_p^2 \rho_p u_r C_c}{18 \mu_{wg} d_d} \tag{3.12}$$

The Cunningham correction factor is taken into account if the particle size is smaller than 15 µm (0.015 mm). For larger sized particles, the factor is approximately 1.33.

In direct contact condensers heat and mass transfer surface is formed by inlet water droplet and gas phase transfer surface, which is variable and mainly dependent on flow hydrodynamic regimes. As a result of increased moisture content and low water temperature, intensive vapour condensation on droplet surface occurs and its diameter increases, the gas moisture content decreases. Wet gas flow is considered as a mixture of dry gas and water vapour flows. Gas moisture content is the ratio of wet gas water vapour mass to dry gas mass:

$$\omega = \frac{m_v}{m_{dg}} = -\frac{\Delta m_g}{m_{dg}} = \frac{\Delta m_w}{m_{dg}}, \text{kg/kg}_{\text{dg}} \tag{3.13}$$

The driving force of the condensation process is the difference between the partial pressure of vapour flow and saturation pressure on water droplet surface. Moisture condensation on water droplet surface changes its mass. The condensate changes in the unit are obtained by multiplying both sides of the equation by the number of droplets. Taking into account the relationship between the condensate changes and moisture content (3.13), the final equation for moisture content calculation is obtained:

$$\frac{d\omega}{dZ} = -\frac{6 V_w \beta_p d_d^2 M_v (p_b - p^{sat})}{d_{d_0}^3 u_d m_{dg}}, \text{kg/kg}_{\text{dg}} \tag{3.14}$$

Contaminated gases are let into the lower part of the FU and they move upwards. Water, in a form of droplets, moves opposite the gas flow. When droplets collide with PM, particles are captured and the PM concentration in wet gas flow is reduced. To evaluate the PM capture efficiency, the particulate amount, which simultaneously fills the volume of the unit – holdup, must be known. Holdup is affected by the sprayed water amount and movement velocity of particles in the unit. The sprayed water amount is determined by water-gas volume ratio. For the PM_{10} capture, if droplet size is from 0.5 mm to 2.0 mm, this ratio is recommended [32] to be from 0.7 l/m^3 to 2.7 l/m^3. Experimental studies performed by Bashir Ahmed Danzomol, et al. show that an optimal PM capture is observed if the droplet diameter is 0.5 mm and water-gas ratio is 2.7 l/m^3. The ratio can be expressed as 0.0027 V_w, m^3 / V_g, m^3. It has to be noted that holdup describes a situation where velocity is constant. If the gas flow is constant, then concentration changes can be determined as in [32]:

$$\frac{C_{p\,iz}}{C_{p\,ie}} = exp\left(-\frac{1.5G_w u_r Z \eta_d}{V_{wgp}(u_r - u_{wg})d_d}\right) \tag{3.15}$$

It should be noted, that velocity of particles varies, because the gas flow in the unit changes due to vapour condensation from wet gases to droplets. Velocity of particles also changes with the changes in gas temperature. If it is assumed that the change in gas flow is related only to the change in temperature, then using the gas state equation, it can be written as

$$\frac{dV_g}{V_g} = \frac{dt_g}{t_g} \tag{3.16}$$

By taking into account the last equation, concentration changes in the unit can be expressed as

$$\frac{dC_p}{dZ} = -= -\frac{1.5C_p u_r \eta_d V_w d_d^2}{u_d d_{d_0}^3 V_g} - \frac{C_p dt_g}{(273+t_g)}, \mathrm{kg/(m^3 \cdot m)} \tag{3.17}$$

This equation should consider that assumptions are made: changes in gas flow due to vapour condensation and PM capture are not considered.

Heat and mass transfer between droplets and wet contaminated gas flow

If heat and mass transfer occurs between droplets and gas, then the droplet temperature changes. Changes can be determined by looking at the heat balance equation of a droplet, which relates to the change of droplet's heat in the direction of *Z* axis with heat transferred by heat exchange, the heat of wet gas vapour condensation and the heat supplied by captured PM:

$$\frac{dQ_d}{dZ} = \frac{dQ_{ht}}{dZ} + \frac{dQ_c}{dZ} + \frac{dQ_p}{dZ}, \mathrm{J/(s \cdot m)} \tag{3.18}$$

The temperature of droplets in the direction of Z axis decreases. The temperature of the gas flow changes in relation to the heat exchange caused by heat transfer with water droplets, the water vapour mass transfer to droplets and heat transfer from gas to droplets with captured PM. The surface of all droplets has to be taken into account because the contact between both heat carriers occurs through it. The number of droplets in the unit must be known.

Variable n_d determines, how many droplets are in the unit at a certain time. Assuming that droplets do not merge or divide, but only their mass and volume increases, then the number of droplets can be determined by dividing the sprayed water volume flow with the initial volume of a droplet. Based on a number of droplets in the unit in one second, the total number of droplets in the volume of the unit is calculated:

$$n_{sk} = \frac{6V_wH}{\pi d_{d_0}^3 u_d} \tag{3.19}$$

Using the number of droplets, temperature changes in the element can be expressed from gas flow heat balance:

$$\frac{dt_g}{dZ} = \frac{6V_w d_d^2}{d_{d_0}^3 u_d m_g c_{pg}}\left[-\alpha(t_g - t_d) - \beta_p M_v c_{pv}(p_b - p^{sat})(t_g - t_d) - \frac{1}{4}C_p u_r \eta_d c_{pp}(t_g - t_d)\right] \tag{3.20}$$

The Ranz and Marshall correlations, proposed in study [33], are used for the calculation of heat and mass transfer coefficient:

$$Nu = \frac{\alpha d_d}{\lambda_g} = 2 + 0.6Pr^{1/3}Re^{1/2} \tag{3.21}$$

$$Sh = \frac{\beta_c d_d}{D_v} = 2 + 0.6Sc^{1/3}Re^{1/2} \tag{3.22}$$

The following equations are usedf for calculations of similarity numbers:

$$Re = \frac{\rho_g u_r d_d}{\mu_g} \tag{3.23}$$

$$Pr = \frac{\mu_g c_{pg}}{\lambda_g} \tag{3.24}$$

$$Sc = \frac{\nu_g}{D_v} = \frac{\mu_g}{D_v \rho_g} \tag{3.25}$$

3.3. Implementation algorithm of the model

The main results of the model are parameter changes in the unit described by six base equations:

$$\frac{dt_g}{dZ} = \frac{n_{sk}\pi d_d^2 \Delta Z}{u_d m_g c_{pg}}\left[-\alpha(t_g - t_w) - \beta_p M_v c_{pv}(p_b - p^{sat})(t_g - t_w) - \frac{1}{4}C_p u_r \eta_d c_{pp}(t_g - t_w)\right] \quad (3.26.)$$

$$\frac{dt_w}{dZ} = \frac{n_{sk}\pi d_d^2 \Delta Z}{V_w \rho_w c_{pw} u_d}\left[-\alpha(t_g - t_w) - \beta_p M_v (p_b - p^{sat})[r + c_{pv}(t_g - t_w)] - 1{,}5C_p u_r \eta_d c_{pp}(t_g - t_w)\right] \tag{3.27}$$

$$\frac{dd_d}{dZ} = -\frac{2\beta_p M_v (p_b - p^{sat})\Delta Z}{\rho_w u_d} \tag{3.28}$$

$$\frac{du_d}{dZ} = -\frac{3C_D u_r \mu_g Re \Delta Z}{4\rho_w d_d^2 u_d} + \frac{g\Delta Z}{u_d} \tag{3.29}$$

$$\frac{dC_p}{dZ} = -\frac{n_{sk} 0.25 C_p u_r \eta_d \pi d_d^2 \Delta Z}{u_d V_g} + \frac{C_p dt_g}{(273 + t_g)} \tag{3.30}$$

$$\frac{d\omega}{dZ} = -\frac{n_{sk}\beta_p \pi d_d^2 M_v (p_b - p^{sat})\Delta Z}{u_d m_{dg}} \tag{3.31}$$

The programme that includes the calculations model of the FU is written in *PYTHON 3.7* using *Visual Studio 2019*. The main parameters, whose changes are studied in the model, are: sprayed water temperature, flue gas temperature, sprayed water droplet diameter and velocity, PM concentration and gas moisture content. Using the obtained model data, the capacity of the FU is calculated. The assumptions made during the development of the model are described in Subchapter *3.1. Droplet movement in wet gas flow in condensation*. The programme has several iteration cycles. The calculations include four main sets of activities:

1) calculation of thermophysical parameters at height Z;
2) calculation of *Re* numbers;
3) calculation of an individual element;
4) parameter change calculations at the output of an element.

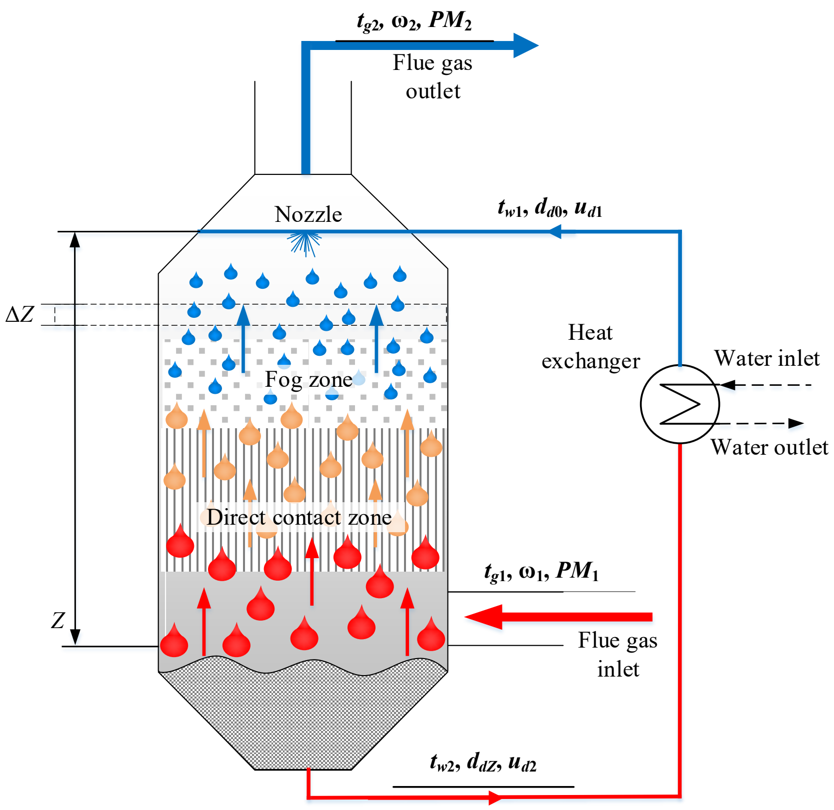

Fig. 3.1. The operation principle of the model in the scheme of the fog unit

Calculations are repeated until parameters are determined in the full height of the unit and changes in water temperature and droplet diameter are applicable to determined range of changes (see Fig. 3.2). Calculations are performed in the following steps:

1) sensor measurements and constants are entered;
2) the height of element Δ*Z* (change step of parameters) is determined;
3) initial values of water droplet diameter and temperature in the calculations are determined;
4) limits for differences of water droplet diameter and temperature with input data are set;
5) thermophysical parameters at specific height *Z* are calculated;
6) *Re* value at input is assumed;
7) actual *Re* value at specific conditions is calculated;
8) difference limits for actual and assumed *Re* values are determined;
9) calculations of elements are continued using calculated *Re*;

10) calculations for parameter changes at the output of an element (performed at the height of the unit until $Z \geq H$, where H is the full height of the unit);
11) verification that the water temperature and droplet diameter correspond to the input data;
12) output of main results, which are summarized in a *csv (comma-separated values)* file.

Calculations of thermophysical parameters include heat capacity, density, dynamic viscosity, calculations of thermal conductivity coefficients for flue gas components, calculations for diffusion coefficient between environments for heat of water phase change. In addition, different numbers describing heat and mass transfer are calculated, for example, the *Pr* number. Equations that describe PM capture in water as well as change calculations in elements are included. The main output data are flue gas temperatures, water temperatures, changes in droplet diameter, droplet velocity, PM concentration and flue gas moisture.

Sensor measurements and expected results are entered in an input file according to given instructions. When starting the programme, a window opens, displaying the final part of calculations. The results of the programme are automatically saved in a *csv* file. In addition, the programme offers to display interactive graphs, which can be enlarged, reduced or zoomed in.

The size of an element, for which calculation will be made, has to be determined in an input data file. Constants have to be input, that include the height of the boiler, molar masses of CO_2, N_2 and H_2O, gas constant and gravitational acceleration. Variables not included in the cycle, but necessary for calculations of thermophysical parameters, and obtained in experiments, are: CO_2, dry gas, N_2, vapour and gas mass flows; air consumption coefficient; atmospheric pressure; diameter and density of a particle.

Variables included in the cycle, that are obtained during experiments, are inlet flue gas and water temperatures, inlet water droplet diameter, inlet flue gas moisture content and mass, inlet flue gas velocity and PM concentration, as well as flue gas volume.

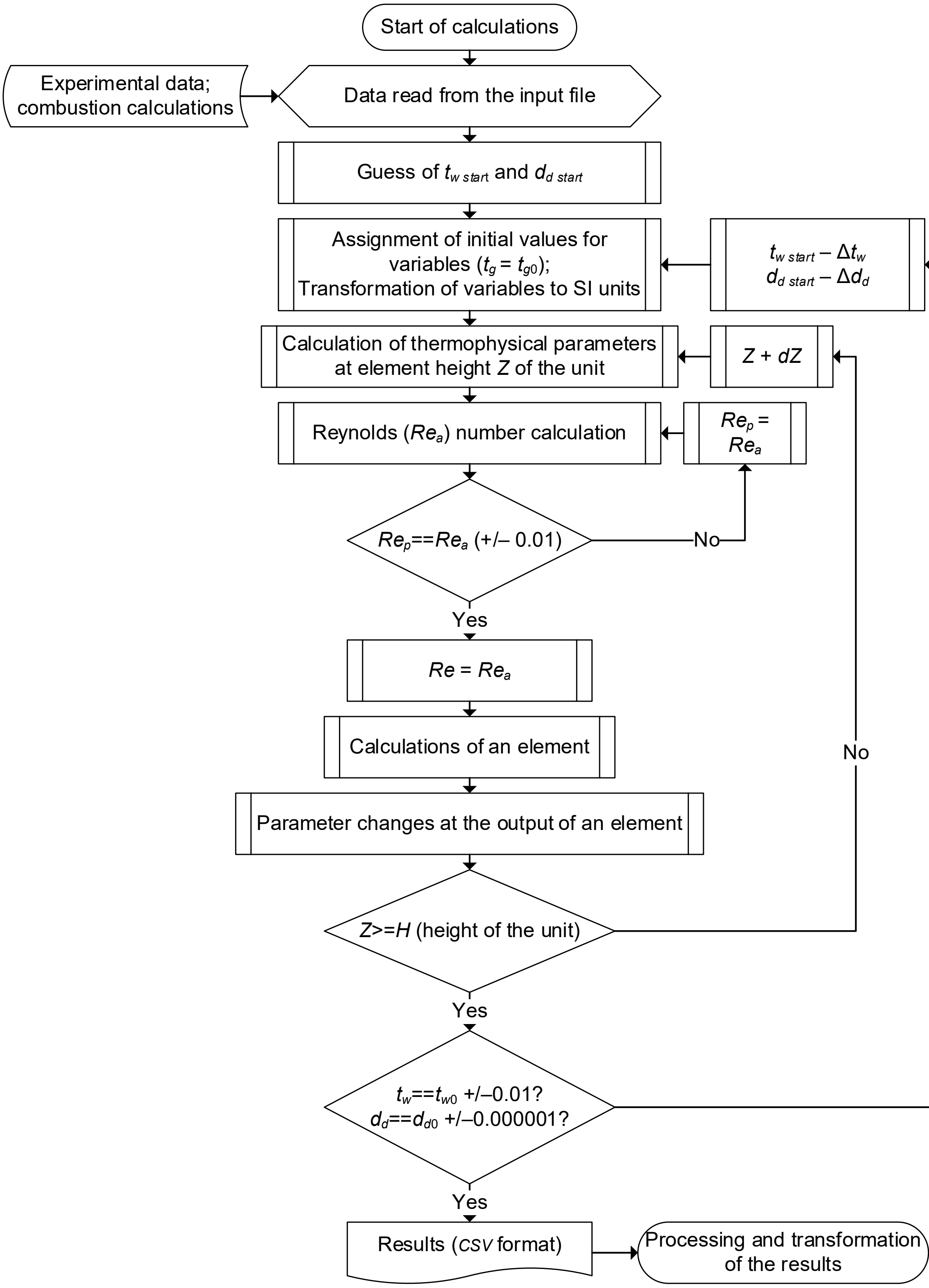

Fig. 3.2. Calculation algorithm of the developed model

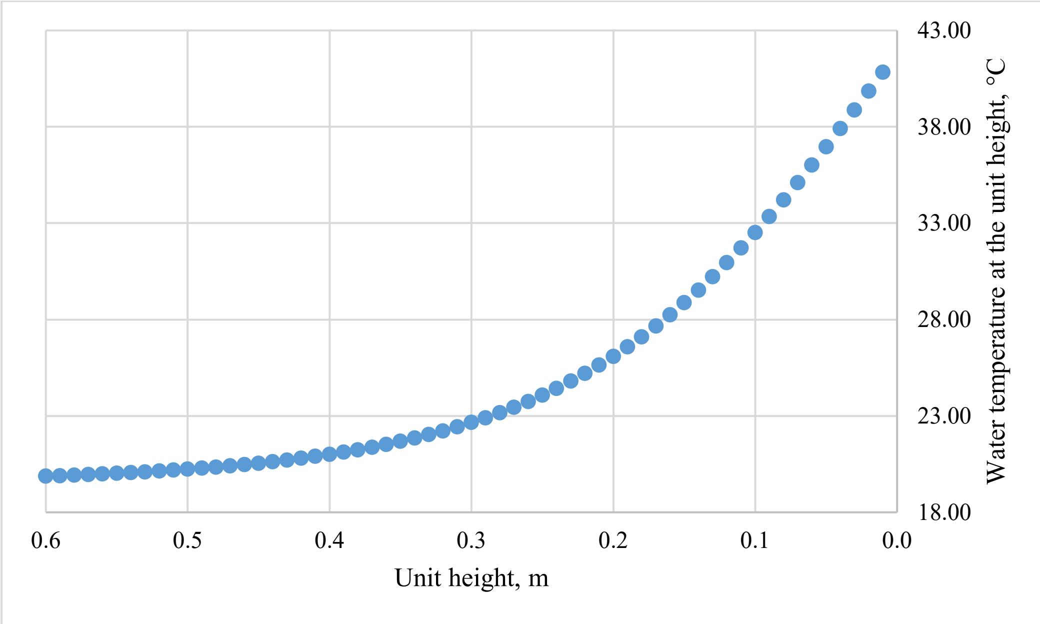

Fig. 3.3. Modelled sprayed water temperature changes in the unit height

Output data are displayed in the full height of the unit, for example, if the unit height is 0.6 m and element height is 0.01 m, then parameter changes are studied in 60 elements. An example for sprayed water changes in the unit height are shown in Fig. 3.3. Water is sprayed in the upper part of the unit, therefore, temperature increases when water moves lower. In this case, a regime was modelled at 20 kW boiler capacity, sprayed water flow rate of approximately 150 l/h and sprayed water temperature of around 20 °C.

4. RESULTS

The FU system experiments were performed using a pellet boiler with options to change operation parameters to reach capacities from 10 kW to 30 kW. Three nozzles of different sizes were used for water spraying: *MPL 0.77*, *MPL 1.12,* and *MPL 1.51*. These nozzles are durable against clogging, and they can be used with water having a small particulate matter addition.

4.1. Results of experimental stand verification

The main variable parameters in experiments are sprayed water amount (flowrate, G, l/h), water temperature at the inlet of the condenser (t_{w1}, °C) and intitial droplet diameter (d_{d0}, μm). Droplet diameter is strongly related to the nozzle parameters (spraying pressure, nozzle size). Flue gas temperatures are related to capacity of the boiler and oxygen content in flue gases.

Table 4.1

Results of Experiments at Pellet Boiler Capacity of 20 kW and Tested Nozzles

Parameter/ Nozzle	***MPL 1.51***	***MPL 1.12***	***MPL 0.77***
G, l/h	49.2–250.3	51.8–252.5	49.0–201.3
t_{w1}, °C	19.7–40.5	19.7–40.9	19.4–39.8
Q, kW	0.51–2.56	0.50–2.63	0.52–2.49
d_{d0}, μm	297–503	263–457	249–379
t_{g1}, °C	130.8–135.2	130.8	130.8
t_{g2}, °C	28.6–77.6	28.0–74.2	29.0–70.4
O_2, %	10.9–11.3	10.2–11.6	10.7–11.7
$C_{p\,i}$, mg/Nm^3	36.2	36.2	36.2
$C_{p\,o}$, mg/Nm^3	8.2–22.8	8.2–24.2	10.4–26.3
ΔC_p, %	37.0–77.2	33.1–77.3	27.2–71.2
Number of experiments	9	9	9

Experiments using all nozzles were perfomed at pellet boiler capacity of 20 kW. PM concentration before the unit in all cases was measured in separate experiments and the average obtained concentration was assumed as reference value because the boiler is operating at the same operation conditions. Droplet diameters were obtained according to the calculations given by the producer of the nozzles. For nozzle *MPL 1.51* they range between 297 μm and 503 μm. Flue gases in experiments were cooled down to 28.6 °C. The most efficienct flue gas cooling was observed at the lowest sprayed water temperature and largest sprayed water flowrate. However, in this case, droplet outflow from the unit – in flue gas ducts – was also observed.

In experiments using the middle nozzle *MPL 1.12* droplet diameters were between 263 μm and 457 μm. Flue gases in experiments were cooled down to 28.0 °C. The most efficient flue gas cooling was observed at the lowest sprayed water temperature and largest sprayed water flowrate. However, droplet outflow from the unit was observed once more. In all experiments at 20 kW boiler capacity oxygen concentration in flue gases was approximately 10–12 %, therefore, small changes in flue gas temperatures before the FU were observed.

In experiments using the smallest nozzle *MPL 0.77* the droplet diameters were between 249 µm and 376 µm. Flue gases in experiments were cooled down to 29.0 °C. The most efficienct flue gas cooling was observed at the lowest sprayed water temperature and largest sprayed water flowrate. Droplet outflow from the unit was observed here as well (see Fig. 4.1).

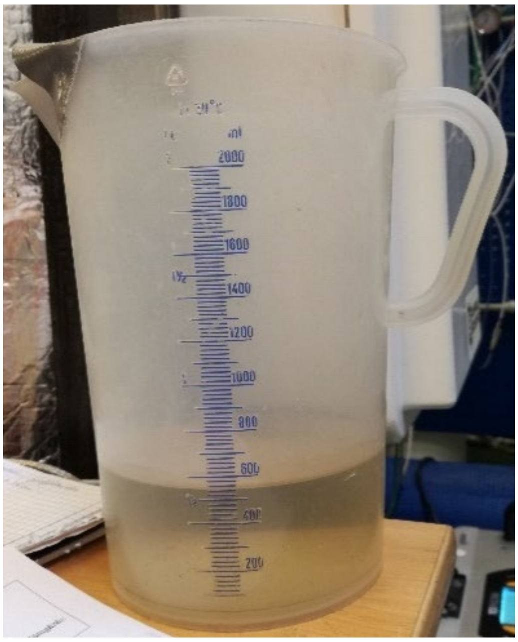

Fig. 4.1. Water discharged from the particulate matter measurement point in the flue gas duct

Droplet outflow outside the FU was observed when the sprayed water flowrate exceeded 200 l/h. At PM measurement point in a flue gas duct after the condenser, a pipe to discharge excess water was inserted, and during experiments a significant water build-up in the system after the FU was observed. Figure 4.1 shows the amount of water discharged from the flue gas duct during one test (30 minutes). Another thing observed in these cases was dissolving of PM measurement filters due to high moisture content in flue gases.

The most efficient flue gas cooling was observed at larger sprayed water flowrates. In this case, the most intensive droplet outflow outside the unit was also observed. These experiments served as verification of the unit operation at different operation parameters of the boiler. Based on obtained results, the main spraying nozzle was selected, which offers an opportunity to provide a wide range of water flowrates and potentially the highest efficiency at different boiler capacities.

4.2. The fog unit performance test results

The performance tests of the FU were carried out in laboratory conditions close to the actual conditions observed in households. The fuel used in experiments was wood pellets of the highest quality class. The nozzle used for water spraying in the unit was *MPL 1.51*, which provides the optimal flowrates and droplet diameters ranging from 224 µm to 509 µm depending on the pressure on the nozzle outlet. The specific nozzle was selected based on experimental results of system verification at different conditions. Parameters of the system at verified capacities are summarised in Table 4.2.

Table 4.2

Parameters of the Fog Unit System at Different Boiler Capacities

	10 kW	**20 kW**	**30 kW**
O_2 in flue gases, %	7.5–10.9	10.4–11.2	7.6–10.9
Sprayed water amount, l/h	45.5–160.2	49.2–240.9	261.5–341.7
t_{w1} before the FU, ºC	19.4–19.9	19.7–20.2	19.6–20.3
t_{w2} after the FU, ºC	24.9–29.4	28.9–34.3	29.9–35.2
Recovered heat, kW	0.5–1.1	0.7–2.6	4.1–5.2
The energy efficiency of the FU, %	3.7–8.8	3.2–10.8	11.1–14.5
The total efficiency of the system, %	89.2–97.0	87.6–97.7	95.0–96.8
PM before the FU, mg/Nm^3	52.6–69.3	36.2	59.1–106.6
PM after the FU, mg/Nm^3	17.1–35.5	15.5–24.2	28.9–44.8
PM capture efficiency, %	48.8–67.5	33.157.1	45.5–67.9
Flue gas parameters			
t_{g1} before the FU, ºC	87.5–97.0	130.8–135.2	157.9–180.6
Relative moisture content before the FU, %	2.4–3.2	2.4–3.2	2.4–3.2
t_{g2} after the FU, ºC	29.1–52.1	28.6–74.1	30.3–36.2
Relative moisture content after the FU, %	45.1–85.6	16.0–89.2	89.5–92.3
Absolute moisture content after the FU, g/kg$_{dg}$	22.1–50.9	22.1–38.8	25.8–36.2
Pressure difference after the FU, Pa	–9.2 to –22.0	–11.6 to –20.7	–15.0 to –19.9

In addition, based on verification results of the system, it was concluded that the highest results of condenser's operation can be achieved by spraying water with the lowest temperature (approximately 20 °C) in the FU. Therefore, the performance tests were not carried out at water temperatures of 30 °C and 40 °C. The results summarised in Table 4.2 describe the overall situation at each of the tested boiler capacities. The energy efficiency of the FU was calculated using Equation (4.1), where the average duration of an experiment – 30 minutes or 0.5 h, is included:

$$\eta_{fu} = \frac{Q \times 0.5}{Q_{con}} \times 100 \quad (4.1)$$

Data shows that the smallest PM reduction is at 20 kW boiler capacity. It is related to boiler operation at nominal or optimal conditions where the initial PM concentration is low, approximately 36.2 mg/Nm^3, therefore, it is hard to achieve the highest PM capture efficiency, because by actual numbers 15.5–24.2 mg/Nm^3 is already a very low concentration. The total efficiency of the system is between 87.6 % and 97.7 %. The highest and the lowest efficiency of the system is achieved at 20 kW boiler capacity.

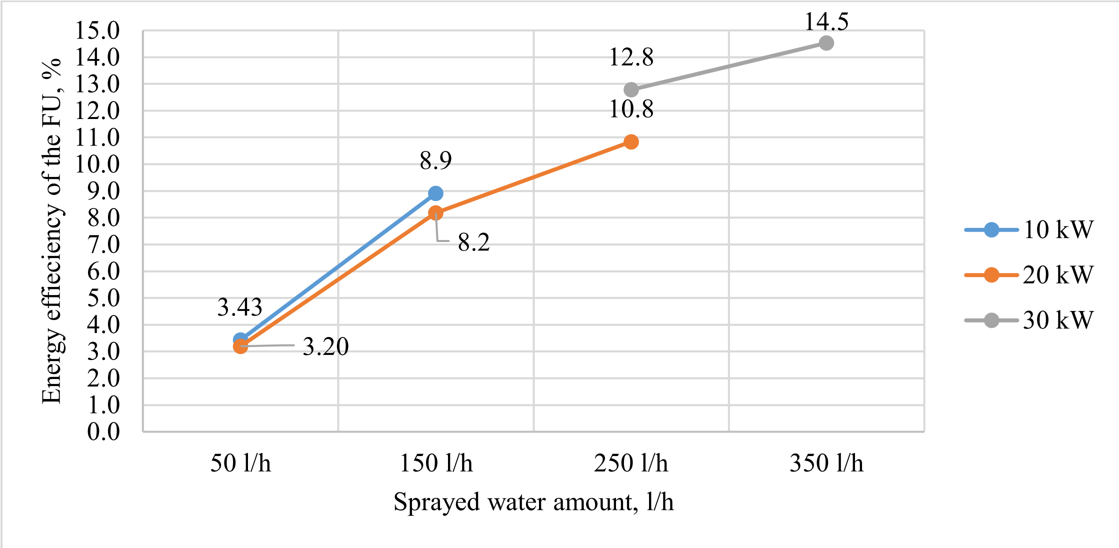

Fig. 4.2. The energy efficiency of the fog unit depending on sprayed water amount at specific oxygen content in flue gases

Figure 4.2 shows energy efficiency achieved in the FU at the oxygen content in the flue gas ~11 % at each of the considered capacities, depending on the sprayed water amount. The highest FU efficiency – 14.5 % – is achieved at a boiler capacity of 30 kW, in which case the highest sprayed water amount is used – approximately 340 l/h. Meanwhile, the lowest FU efficiency – 3.2 % – is observed at a capcity of 20 kW and the sprayed water amount of about 50 l/h. It is important to note that as the boiler capacity increases, the flue gas temperature also increases. In the case under consideration, the temperature in the flue gas before FU varies from 88 °C to 97 °C at a boiler capacity of 10 kW, while at a boiler capacity of 30 kW, it varies between 158 °C and 181 °C, depending on the amount of air supplied to the boiler and the concentration of oxygen in the flue gas.

As the flue gas temperature increases, heat losses caused by outgoing flue gases also increase. As a result, an amount of heat that can additionally be recovered by the FU is carried away by the flue gas. In fact, this means that the higher the flue gas temperature before the FU is, the potentially higher the energy efficiency FU can achieve. In the case where the sprayed water amount exceeds 200 l/h, a significant water outflow outside of the FU is observed. This observation led to the insertion of a filling – metal shavings – into the FU, in addition to excluding larger sprayed water amounts from subsequent experiments. The results of PM concentrations before the FU are additionally influenced by the characteristics of the boiler – changes in the efficiency depending on the selected operation parameters. The highest efficiency of the boiler is achieved at the nominal boiler power, which in this case is 20 kW. The efficiency of the boiler of the tested system, depending on the selected operation capacity, ranges from 82.3 % to 88.0 %, the lowest efficiency shown at 30 kW, and the highest at 10 kW boiler capacity. The overall achieved efficiency of the system, considering the efficiency achieved by the boiler and the FU, varies from 87.6 % to 97.7 %, which increases the overall efficiency of the system in any case and confirms the efficiency and functionality of the FU in the system.

The data of the experiments are further analysed to determine the interaction of parameters. Figure 4.4 shows the change in the FU capacity depending on the flue gas flow rate. The FU capacity increases with increasing flue gas and sprayed water flows, while the capacity reduction is most directly affected by the sprayed water temperature. A moderately close correlation is observed between the flue gas flow and the FU capacity, the determination coefficient is around 0.58. The trend of correlation is characterized by the polynomial equation, which is also presented in the graph.

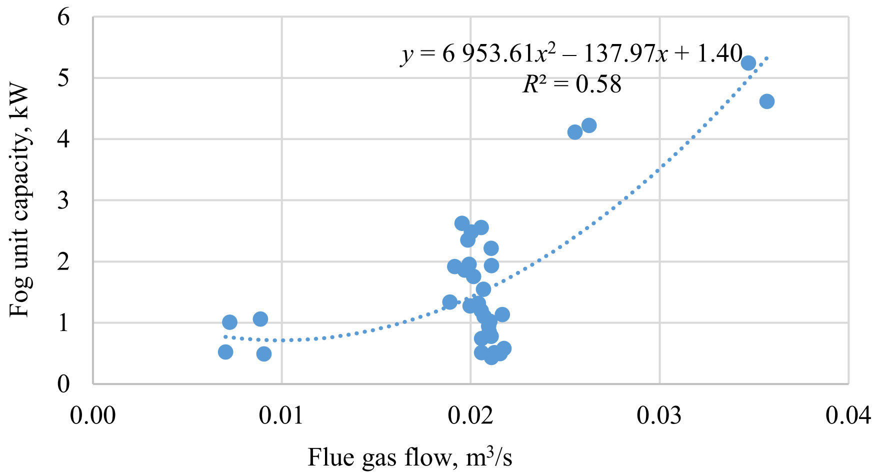

Fig. 4.3. Fog unit capacity depending on the flue gas flow

Regression analysis is carried out not only for the FU capacity influencing parameters, but also for interrelated key parameter data. As seen in Fig. 4.4, when searching for a mathematical relationship between the temperature of the flue gas at the outlet of the FU and the initial diameter of the water droplets, a moderately close correlation between the data is obtained, the determination coefficient is 0.64. In the given case, a linear relationship is obtained, which is also reflected in the figure.

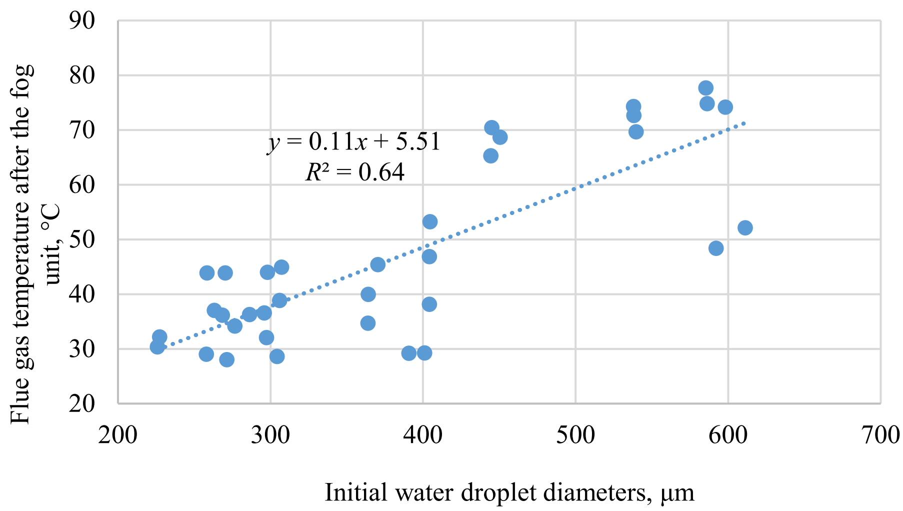

Fig. 4.4. Flue gas temperature after the fog unit depending on intitial water droplet diameter

Higher flue gas temperature after the FU is observed in cases where the temperature of the sprayed water is higher and the diameter of the droplets is larger. At higher flue gas temperatures, there is a strong data dispersion.

By increasing the sprayed water amount, the water temperature at the FU outlet and throughout the unit increases. That is, the difference between the temperatures of flue gases and water also increases, and convective heat exchange becomes more intense. In order to increase the sprayed water amount, it is necessary to increase the pressure on the nozzle and thus ensure smaller droplet diameters, as seen in Fig. 4.5.

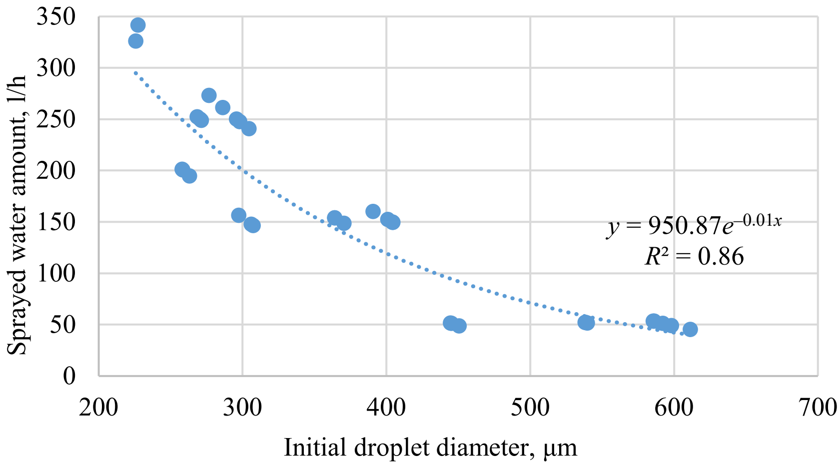

Fig. 4.5. Sprayed water amount depending on initial water droplet diameter

Smaller diameter droplets form a larger phase transition surface. Given the fact that the heat exchange surface in the FU is limited by the diameter of the equipment, this is a logical conclusion. Smaller droplets fill the surface more completely than larger droplets, and flue gases have less ability to move through the surface gaps. Consequently, they have to move through the surface. As a result, both heat and mass exchange improves, and the heat capacity of the FU increases.

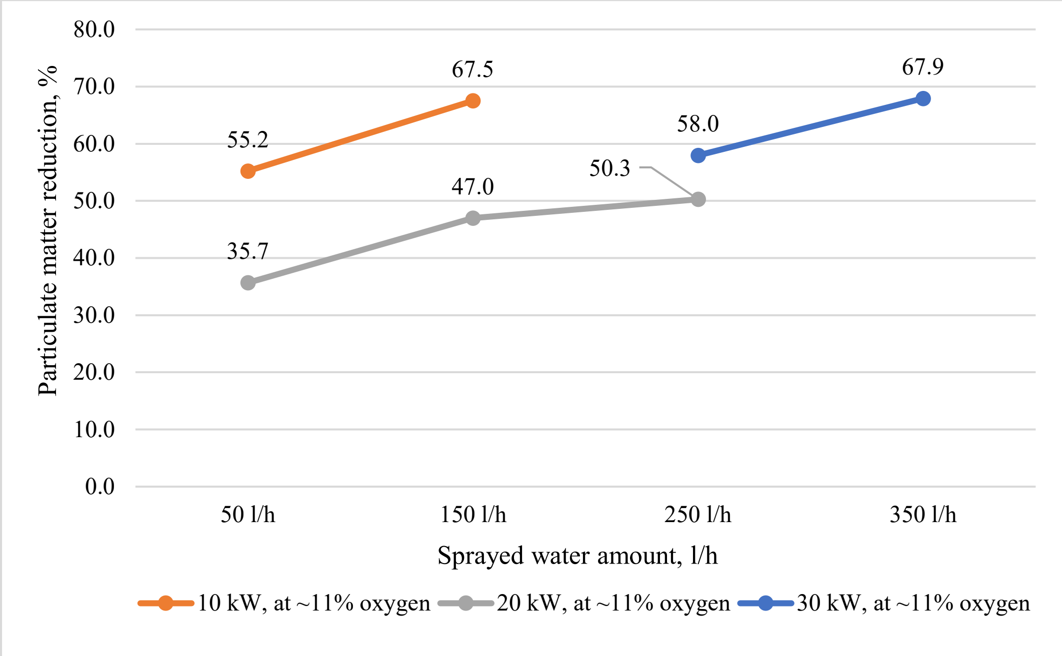

Fig. 4.6. Particulate matter reduction depending on sprayed water amount at different boiler capacities and equal oxygen content in flue gases

The PM level before and after the FU at each boiler capacity is shown in Fig. 4.6. In this case, the data at approximately 11 % of the oxygen content in the flue gases are compared, since experiments have been carried out under these conditions at all considered capacities. At a boiler capacity of 10 kW, the concentration of PM before FU on average is 52.6 mg/Nm^3. In turn, the achieved PM concentration after FU varies from 17.1 mg/Nm^3 to 35.5 mg/Nm^3, achieving a decrease in PM to 67.5 %. The temperature of the sprayed water was around 20 °C in all tests at a given capacity. As shown in the figure, the greatest decrease in PM concentration is achieved with the largest sprayed water amount.

The average PM concentration before FU for a boiler operating at a capacity of 20 kW is 36.2 mg/Nm^3. In turn, the achieved PM concentration after FU at this boiler capacity is on average in the range of 18.0 mg/Nm^3 to 23.3 mg/Nm^3, achieving a decrease in PM around 50.3 %. The greatest decrease in PM concentration after FU in the considered regimes is observed at the sprayed water temperature around 20 °C and the sprayed water amount of ~250 l/h. The lower decrease in PM at 20 kW boiler capacity is observed for two reasons: First, the concentration of PM before FU is constant in all cases; secondly, tests at 10 kW and 30 kW were carried out after the improvement of the FU – the introduction of a water separator to reduce the outflow of water droplets after the unit. At a boiler capacity of 30 kW the PM concentration before FU is 106.6 mg/Nm^3 at an oxygen concentration in the flue gas of 11 %. The greatest decrease in PM – 67.9 %, is achieved at the sprayed water amount of ~350 l/h.

Based on the conducted FU system tests in an artificially created environment, it can be concluded that the effectiveness of PM capture depends not only on the parameters of the FU operation, but also on the initial concentration of PM. In general, the concentration of PM behind the boiler or before FU is lowest at a capacity of 20 kW – 36.2 mg/Nm^3. At 10 kW boiler capacity, the PM concentration after the boiler is 52.6 mg/Nm^3 and 69.3 mg/Nm^3, depending on the oxygen concentration in the flue gas. In turn, at 30 kW boiler capacity, the PM concentration behind the boiler is 59.1 mg/Nm^3 and 106.6 mg/Nm^3, depending on the oxygen concentration in the flue gas. These results can be explained by the fact that all experiments were carried out with one boiler, changing its capcity through fuel consumption. The nominal capacity of the boiler is 20 kW, at which the highest efficiency and the most complete combustion of fuel is achieved. When the boiler is working at reduced capacity, the furnace temperature and efficiency decreases and the emission concentration increases. When the boiler works at increased capacity, the amount of flue gas generated increases significantly. This results in an increased flue gas flow rate. This negatively affects the heat exchange, resulting in a decrease in the efficiency of the boiler. In addition, fuel fed into the boiler at increased flue gas flows combust incompletely, increasing the concentration of emissions. The results of the experiments confirm this.

Analysis of the performance of the experimental stand suggests that it is possible to carry out effective PM capture with the developed system. However, the system has its limitations. Experimental data indicate that the PM concentration in the flue gas can be reduced to 10–20 mg/Nm^3 at optimal FU operation parameters. Since the EU Ecodesign Directive states that for small capcity boilers with automatic fuel feed, such as a pellet boiler in an experimental stand, PM emissions must not exceed 40 mg/m^3, this concentration is considered to be sufficiently low. This shows that thanks to FU technology it is possible to achieve twice the concentration of PM than required. It should be taken into account that in cases where the concentration of PM before FU is already initially low (36.2 mg/Nm^3 at a boiler power of 20 kW), the decrease in PM is lower. However, the opposite situation is observed at higher boiler capacities, for example, with an initial PM concentration of 106.6 mg/Nm^3 at a boiler capacity of 30 kW it is possible to achieve a reduction of up to 34.2 mg/Nm^3.

4.3. Validation of the calculations model

The validation of the calculation model was performed using a comparison of experimental and model results. A similar validation method comparing modelled and experimental data is widely used to characterize heat and mass transfer processes. Zheng et al. [34] developed a numerical algorithm to characterize the droplet dynamics in wet air droplet condensation and applied the algorithm to the entire condensation process. An individual droplet growth model was developed in the study and was attributed to a limited surface area. To validate the results, drop condensation experiments were performed at 94 % and 80 % relative humidity. A good agreement was obtained between the results of the model and the experiment, proving the reliability of the model.

The FU capacity values obtained with the model were compared with the experimental results in the same operating regimes. Data from 16 experiments and the results of the corresponding experimental regimes obtained from the calculation model were compared. The difference in results was calculated using the capacity of the FU from the experiments as reference values in Equation (4.2):

$$\Delta Q = \frac{(Q_{exp.} - Q_{calc.})}{Q_{exp.}} \times 100. \quad (4.2)$$

Table 4.3

The Main Parameters of the Research

No.	t_{w1} exp. ~ t_{w1} calc. °C	t_{w2} exp. °C	t_{w2} calc. °C	G l/h	Q exp. kW	Q calc. kW	ΔQ %
1	20.2	33.2	33.2	49.2	0.75	0.77	–2.96
2	19.7	30.8	31.0	150	1.93	2.07	–7.09
3	30.5	38.8	38.8	53.4	0.51	0.53	–3.15
4	29.4	36.7	36.6	150	1.28	1.32	–3.66
5	39.5	46.5	46.5	53.7	0.44	0.44	–1.16
6	40.0	45.5	45.5	150	0.95	0.99	–4.08
7	20.1	34.3	34.2	51.8	0.85	0.87	–2.08
8	19.9	32.3	32.5	154	2.22	2.41	–8.70
9	19.7	27.4	28.0	249	2.63	2.40	8.69
10	30.3	39.9	39.9	52.3	0.58	0.60	–3.20
11	29.9	38.6	38.6	154	1.55	1.64	–5.74
12	40.9	49.1	48.4	52.4	0.50	0.45	**9.08**
13	39.9	46.2	46.3	149	1.11	1.15	–4.05
14	19.4	38.2	38.4	51.8	1.13	1.18	–3.93
15	30.3	44.0	43.9	49.0	0.78	0.80	–1.75
16	29.9	40.1	40.4	148	1.76	1.91	–8.83

The main parameters used in the comparison are summarized in Table 4.3. Input parameters from the experimental data are flue gas temperature after the boiler (t_{g1}), inlet water temperature (t_{w1}), sprayed water flowrate (G), and the initial water droplet diameter (d_{d0}). The results of experiments used for validation were at 20 kW boiler capacity because it is the nominal capacity of the boiler that is used in experiments. The flue gas temperature after the boiler was the same in 15 regimes (131 °C), while the temperature in one regime was 135 °C, therefore, the flue gas temperature is not included in the data table. Three different nozzles were used in the experiments, which provide similar water flowrates with different droplet diameters. The amount of sprayed water is between 50 l/h and 249 l/h. Inlet water temperatures ranged from about 20 °C to about 40 °C.

There is a very close correlation between the calculated and experimentally determined water temperatures, which can be seen in Fig. 4.7.

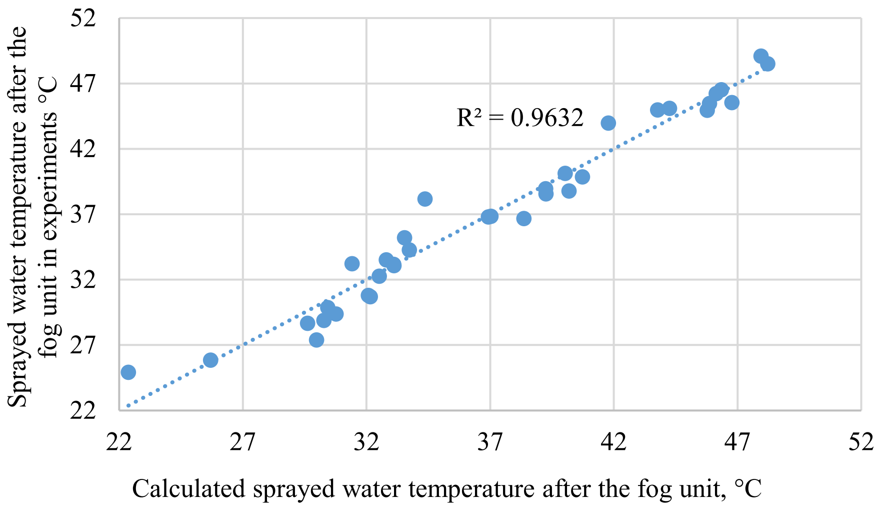

Fig. 4.7. Comparison of the experimental and calculated sprayed water temperatures after the fog unit

It is logical that increasing of the temperature of the sprayed water before the FU will also increase the temperature of the water after the FU. With a closer relationship between the sprayed water amount and the flue gas flow, the temperature of the sprayed water decreases after the FU.

The flue gas temperature after the FU depends on the initial flue gas temperature and water parameters – water temperature after the FU and initial water droplet diameter. As a result of data analysis Equation (4.3.) is obtained:

$$t_{g_2} = -63.08 + 0.20 \times t_{g_1} + 1.03 \times t_{w_2} + 0.12 \times d_{d_0} \tag{4.3}$$

There is a statistically significant relationship between the parameters at the 95 % confidence level. The coefficient of determination is 91.1 %. The experimentally determined water temperatures after the FU were compared with the calculated flue gas temperatures after the FU (see Fig. 4.9).

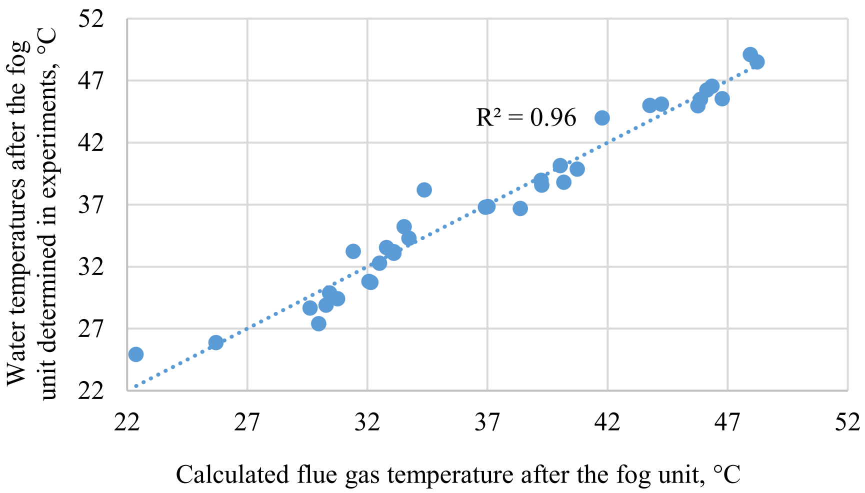

Fig. 4.8. Relationship between water temperature determined in experiments and the calculated flue gas temperature after the fog unit

There is a strong correlation between the data. As the flue gas temperature increases before the FU, the water temperature after the FU will also increase. Similarly, as the water temperature after the FU increases, the flue gas temperature after the FU also increases – the flue gas cooling will be less intense. Increasing the diameter of the water droplets reduces the phase transfer surface and the amount of heat recovered from the flue gas during the convection process. The flue gas cooling will deteriorate, and its temperature will rise.

The capacity of the condenser in experiments ranged from 0.44 kW to 2.63 kW, while the calculated capacity ranged from 0.44 kW to 2.41 kW. The sprayed water amount causes fluctuations in the condenser's capacity values. Elevated inlet water temperature reduces the capacity of the FU, making colder water more suitable for spraying. The sprayed water amount is approximately 150 l/h, which is optimal for heat recovery from flue gases, regardless of the boiler's capacity. To reflect the data and their differences, a graph of the condenser capacities has been made (see Fig. 4.9).

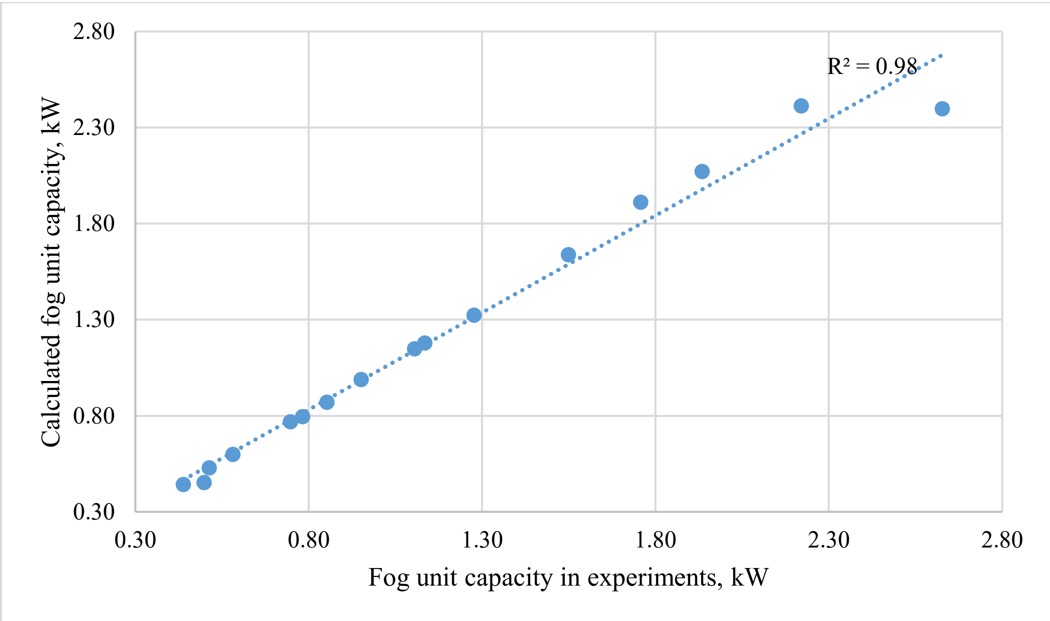

Fig. 4.9. Comparison of the fog unit capacity determined in experiments and calculated by the model

As can be seen in Fig. 4.9, there is a close correlation between the experimental and calculated FU capacities, the determination coefficient is 0.98. As shown in Table 4.3, the largest difference between the calculated and experimentally determined capacity values at water temperature of about 20 °C, with an increasing sprayed water amount, is with an average difference of 8.2 %. The most similar data are at water temperature of about 30 °C, where the sprayed water amount is about 50 l/h (2.7 % on average). The difference between the values ranges from 1.16 % to 9.08 %, with an average difference between data of 4.9 %. As the difference between the data does not exceed 10 %, it is concluded that the modelled data are in good agreement with the experimental data and the model is suitable for the analysis of condenser operation. This analysis includes the experimental results at a boiler capacity of 20 kW using all three nozzle types. At the sprayed water temperature of 30 °C and 40 °C, experiments were performed at the sprayed water amount up to about 150 l/h, to ensure the most efficient PM capture and heat recovery from flue gases, without unnecessary water spraying and possible outflow to flue gas ducts. The experiments at 20 °C highlighted the problems of water outflow and excessive spraying, which were considered and limited in the experiments at higher water temperatures (implementation of a filling to limit water losses, more optimal spraying flowrates).

4.4. Optimisation

Planning of experiments is the development of mathematical calculations with a specific sequence that helps to determine the specific variable of the study [35]. In the mathematical model, in the case of planning of experiments, dependent variable y is used depending on independent variables $x_1, x_2 \ldots x_n$. The real process leads to unpredictable changes in the nature of the case. Thus, regression factors b_0, b_j, b_{uj}, b_{jj} are used. The equation for the changes in variable in general form is displayed in (4.4) [35]:

$$y = b_0 + \sum_{j=1}^{n} b_j x_j + \sum_{\substack{u,j=1 \\ u \neq j}}^{n} b_{uj} x_u x_j + \sum_{j=1}^{n} b_{jj} x_j^2 + \cdots + \epsilon \tag{4.4}$$

In the performed analysis, the dependent variable is the capacity of the FU (Q, kW). Independent variables are:

- flue gas flow (V_g, Nm^3/s);
- flue gas temperature before the FU (t_{g1}, °C);
- the sprayed water amount (G, l/h);
- initial water droplet diameter (d_{d0}, µm);
- sprayed water temperature (t_{w1}, °C).

The analysed flue gas flow range is appropriate for pellet boilers with the capacities of 10 kW to 20 kW and a minimum efficiency of 82 %. The maximum and minimum values of the parameters are determined by analysing the experimental data set and selecting the parameter values to which the calculations model is also applicable. The summary of the main values is shown in Table 4.4.

Table 4.4

Parameter Values of Independent Variables

	V_g, Nm^3/s	t_{g1}, °C	G, l/h	d_{d0}, µm	t_{w1}, °C	ω_1, kg/kg_{dg}	W^d, %
min	0.00482	90	60	425	20		
max	0.01	140	150	600	30	0.08	4.55
vid	0.00735	115	105	512.5	25		

W^d – moisture content of fuel, mass %.

The analysed fuel is wood pellets with a moisture content of 4.55 %. In this case, no specific nozzle is attached to the sprayed water amount and droplet diameters. Since the analysis contains 5 independent variables, the numerical plan of experiments must be composed of

$2^5 = 32$ for experimental regimes, with 3 additional experiments at midpoint values, creating a total number of experiments – 35.

The matrix was created using the *Design of Experiments* tool in the *Statgraphics Centurion XVII* programme. The tool allows to enter the dependent variable *(y)*, independent variables (x_n) and their maximum *(max)* and minimum (min) values, and to choose what type of experiment is planned and how many experiments will be carried out at midpoints (in the 2^k experiment plan, where $k = 1 \dots 5$, 3–5 experiments are usually performed at midpoints). This results in a matrix of variables with different combinations of values indicating the experiments to be performed.

The experiments have been carried out numerically using the developed FU calculation model in the form of the programme. Using the obtained model data, the FU capacity was calculated. The created matrix with the corresponding value label (min, max, avg) and the calculation results of the FU capacity at the respective regimes are summarised in Table 4.5.

Table 4.5

Developed Matrix with Parameter Values and Calculated Fog Unit Capacities

Nr.	V_g, Nm³/s		t_{g1}, °C		G, l/h		d_{d0}, µm		t_{w1}, °C		Q, kW
1	0.01	max	90	min	150	max	425	min	30	max	2.23
2	0.01	max	140	max	150	max	425	min	20	min	3.43
3	0.01	max	140	max	60	min	425	min	30	max	1.66
4	0.00482	min	140	max	150	max	600	max	20	min	1.67
5	0.01	max	90	min	150	max	600	max	20	min	2.47
6	0.00482	min	90	min	150	max	425	min	20	min	1.36
7	0.01	max	90	min	60	min	600	max	30	max	1.08
8	0.00482	min	90	min	150	max	600	max	20	min	1.34
9	0.00482	min	90	min	150	max	600	max	30	max	1.09
10	0.01	max	140	max	150	max	600	max	20	min	3.05
11	0.01	max	140	max	60	min	600	max	30	max	1.34
12	0.01	max	90	min	60	min	425	min	20	min	1.98
13	0.00482	min	90	min	60	min	425	min	20	min	1.31
14	0.00482	min	140	max	150	max	600	max	30	max	1.42
15	0.01	max	140	max	150	max	600	max	30	max	2.50
16	0.00482	min	140	max	60	min	600	max	30	max	1.09
17	0.01	max	140	max	150	max	425	min	30	max	2.90
18	0.01	max	90	min	150	max	600	max	30	max	1.94
19	0.00482	min	140	max	150	max	425	min	30	max	1.44
20	0.01	max	90	min	60	min	425	min	30	max	1.39
21	0.00735	avg	115	avg	105	avg	512.5	avg	25	avg	1.99
22	0.00482	min	90	min	150	max	425	min	30	max	1.10
23	0.01	max	90	min	60	min	600	max	20	min	1.48
24	0.00735	avg	115	avg	105	avg	512.5	avg	25	avg	1.99
25	0.01	max	90	min	150	max	425	min	20	min	2.75
26	0.00482	min	140	max	60	min	600	max	20	min	1.35
27	0.00482	min	140	max	150	max	425	min	20	min	1.69

Table 4.5. continued

Nr.	V_g, Nm³/s		t_{g1}, °C		G, l/h		d_{d0}, µm		t_{w1}, °C		Q, kW
28	0.00482	min	140	max	60	min	425	min	30	max	1.35
29	0.00482	min	140	max	60	min	425	min	20	min	1.63
30	0.01	max	140	max	60	min	425	min	20	min	2.30
31	0.00482	min	90	min	60	min	425	min	30	max	1.05
32	0.00482	min	90	min	60	min	600	max	20	min	1.10
33	0.00482	min	90	min	60	min	600	max	30	max	0.85
34	0.00735	avg	115	avg	105	avg	512.5	avg	25	avg	1.99
35	0.01	max	140	max	60	min	600	max	20	min	1.77

The next step in planning of experiments is the transformation of independent variables into dimensionless values, where variables are labeled as x_1, x_2, x_3, etc. The maximum value of each variable is equal to +1, a minimum is equal to –1. In this case, the results of the midpoints are not taken into account, which means that the variables have been transformed into 32 regimes. The interval and average variable values are obtained by Equations (4.5) and (4.6) [35]:

$$Z_n^0 = \frac{(Z_{n\,max} + Z_{n\,min})}{2} \qquad j = 1, 2, \ldots k \qquad (4.5)$$

$$\Delta Z_n = \frac{(Z_{n\,max} - Z_{n\,min})}{2} \qquad (4.6)$$

The calculated parameter values with assumed coefficients are summarised in Table 4.6.

Table 4.6

Interval and Average Values of Variables

	V_g	t_{g1}	G	d_{d0}	t_{w1}
max	0.01	140	150	600	30
min	0.00482	90	60	425	20
Z^0_n	0.00735	115	105	512.5	25
ΔZ_n	0.00253	25	45	87.5	5
	x_1	x_2	x_3	x_4	x_5

The conversion of coefficients x_1–x_5 to dimensionless coordinates was done according to Equation (4.7). In addition to the analysis, intercept x_0 is introduced, which is +1 in the dimensionless coordinates:

$$x_n = \frac{(Z_n - Z_n^0)}{\Delta Z_n} \qquad (4.7)$$

The next step is to calculate coefficients b_n of variables. Equation (4.8) is used to obtain any coefficient b_n, where the sum of x_{ni} and y_n multiplications is divided by the number of experiments N [35]:

$$b_n = \frac{\sum_{i=1}^{N} x_{ni} y_i}{N} \qquad (4.8)$$

Table 4.7

Coefficient Values of Variables

	x_0	x_1	x_2	x_3	x_4	x_5
$\sum x_n$	55.1274	13.4358	6.0499	9.6420	–4.0206	–6.2705
b_n	1.7227	0.4199	0.1891	0.3013	–0.1256	–0.1960

The obtained equation for dimensionless variables is displayed in (4.9.):

$$\hat{y} = 1.7227 + 0.4199x_1 + 0.1891x_2 + 0.3013x_3 - 0.1256x_4 - 0.1960x_5 \quad (4.9)$$

Once the dimensionless equation is obtained, it is necessary to tranform it to real numbers. x_n is replaced by the variables of experiments. Equation (4.10) is obtained:

$$Q = 1.7227 + 0.4199\frac{V_g - 0.00735}{0.0025} + 0.1891\frac{t_{g1} - 115}{25} + 0.3013\frac{G - 105}{45} -$$
$$-0.1256\frac{d_{d0} - 512.5}{87.5} - 0.1960\frac{t_{w1} - 25}{5} \quad (4.10)$$

The equation of real values (4.11) is obtained:

$$Q = 0.6458 + 165.8865V_g + 0.0076t_{g1} + 0.0067G - 0.0014d_{d0} - 0.0392t_{w1} \quad (4.11)$$

From the dimensionless equation, it can be determined that the variable with the largest effect on the FU capacity is the flue gas flow V_g. To determine whether the equation is adequate to characterize the FU capacity and corresponds to the 95 % confidence limit, a multiple variable regression analysis was performed in *Statgraphics Centurion XVII* (for 32 experimental regimes). As a result of the analysis, the equation describing the FU capacity (4.12) was obtained:

$$Q = 0.6458 + 165.887V_g + 0.0076t_{g1} + 0.0067G - 0.0014d_{d0} - 0.0392t_{w1} \quad (4.12)$$

The obtained adjusted determination coefficient of the regression equation describes 82.26 % of the FU capacity results. Compared to the equation obtained in planning of experiments it can be seen that there are practically no differences between variables. There is no correlation between variables of the equation. This result confirms that the equation obtained in the planning of experiments adequately describes the FU capacity and a separate examination of the statistical significance of the equation variables is not required.

The *BoxWilson* strategy (the gradient method) was chosen for optimisation. The dimensionless equation (4.9) is the reference function of the numerical experiment, and the optimization of the steepest ascent is performed using it. Coefficients of the equation determine the direction of the gradient path and the gradient step. The step is determined by multiplying factor b_i and the proportionality factor γ for each variable. From the dimensionless equation (4.9), the factor that affects reference value y the most is chosen, its change step δ'_k is assumed and proportionality factor γ is calculated. The equation used for calculation is as follows:

$$\gamma = \frac{\delta_k}{\delta_k b_k} \qquad (4.13)$$

The change steps for other factors are proportional to the change steps of the main factor

$$\delta_i' = \gamma \delta_i b_i \qquad (i = 1, 2, \ldots, k) \qquad (4.14)$$

After the first optimisation step, the factor values are calculated as in [36]:

$$x_{in} = x_{i0} + u\delta_i' \qquad (4.15)$$

The aim of optimisation is to find the set of factors that would provide the maximum Q value. The steepest ascent or gradient method was chosen for optimisation. For this purpose, a model that considers only the effects of the main factors (excluding the effects of factor interactions) is used.

In the matrix of numerical experiments, the highest Q value can be reached if $V_g^{\max}$; $t_{g1}^{\max}$; $G^{\max}$; $d_{d0}^{\min}$, and $t_{w1}^{\min}$. This means that in the search for the optimal value, the values of V_g, t_{g1}, G must be increased and d_{d0} and t_{w1} must be decreased. From the regression equation in dimensionless values (4.9) it can be seen that the capacity is affected more by the gas flow, because the coefficient of this factor has the largest value.

The gas flow increase step is selected and, depending on it, the changes in other factors are determined. The optimisation starts in the centre of the numerical experiment. The sequence of the required actions to be performed is shown in Table 4.8. The following regimes defined by the step of factor change in the direction of the steepest ascent are given in Table 4.9.

Table 4.8

Change Steps of Factors in Optimisation

Variables	V_g, Nm^3/s	t_{g1}, °C	G, l/h	d_{d0}	t_{w1}, °C	Q, kW
Centre of the plan	0.00741	115	105	512.5	25	1.755
Change interval	0.00259	25	45	57.5	5	
Upper limit	0.01	140	150	600	30	
Lower limit	0.00482	90	60	425	20	
Coefficients b_i of the dimesionless equation (4.9)	0.4199	0.1891	0.3013	-0.1256	-0.196	
b_i * change interval	0.00109	4.7275	13.5585	-10.99	-0.98	
Change step of a parameter	0.0013	5.62	16.13	-13.078	-1.07	

As shown in Fig. 4.4, the capacity changes of a condenser in generated regimes and the centre of the plan are linear, have no optimum, and the capacity increases with each step. The calculations of the steepest ascent steps presented in Table 4.9 show that for the capacity growth it is necessary to increase the gas flow, increase the sprayed water amount, reduce droplet diameters and spray water at a lower temperature. In the studied equipment, the maximum capacity of the condenser is limited by the flue gas flow of 0.01 Nm^3/s. The flue gas flow is determined by the capacity of the pellet boiler (20 kW) and by the cumbustion of high-quality fuel (oxygen content in the flue gases). Another limitation is the interaction between the gas and droplet flows in the condenser. As the flow increases, the outflow of the smallest droplets from the unit increases.

Table 4.9

Regimes for Determination of the Optimum

	V_g	t_{g1}	G	d_{do}	t_{w1}	Q
1	0.0087	120.6	121.13	499	23.8	2.18
2	0.01	126.2	137.26	486	22.6	2.61
3	0.0113	131.8	153.39	473	21.5	3.05
4	0.0126	137.4	169.5	460	20.33	3.47

The performed reasearch shows that the FU designed for a 20 kW pellet boiler can recover up to 2.6 kW of heat from flue gases. That makes up 13 % of the boiler capacity. In this regime (see Table 4.9) the gas flow must be $V_g = 0.01$ Nm^3/s, gas temperature must be $t_{g1} = 126$ °C, water flowrate must be $G = 137$ l / h, water droplet diameter must be $d_{d0} = 486$ µm, and the sprayed water temperature must be $t_{w1} = 22.6$ °C. The values of reference parameter Q depending on the optimisation step are displayed in Fig. 4.10.

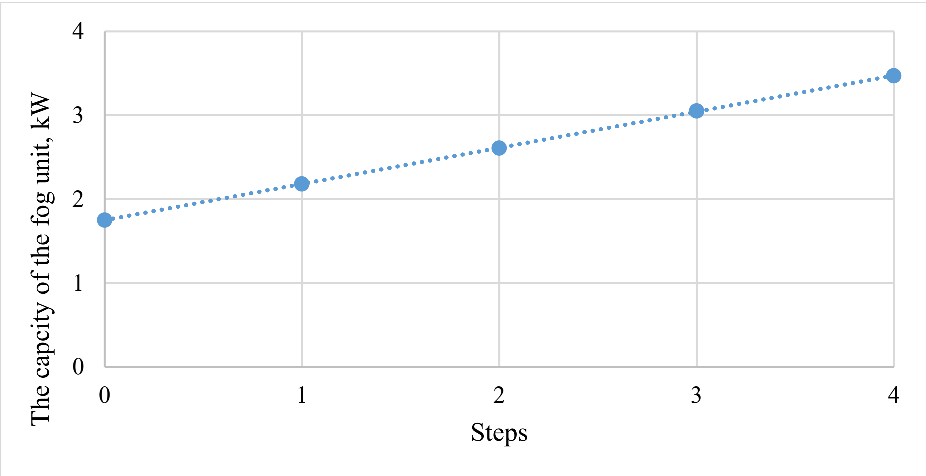

Fig. 4.10. Changes of the fog unit capacity in the direction of the steepest ascent

As the reasearch studies steps in the direction of the steepest ascent, the parameters of each step (regime) are considered as optimal. The values of the optimal regime parameters are shown in Table 4.9. It is important to note that when one selected parameter changes, other parameters change according to a certain regularity, which is described by the regression equation (4.9). Only one parameter can be changed freely. If other change steps are required for optimal operation of the FU, then new step calculations must be performed.

The FU capacity increases as the flue gas flow, flue gas temperature and the sprayed water amount increases and the droplet diameter and sprayed water temperature decreases. In real conditions, the flue gas flow and temperature is dependent on the capacity of the boiler, the fuel used, and the operating parameters of the boiler. The droplet diameter depends on the selected nozzle. Adjustment of the droplet diameter during operation of the FU is limited. The choice and control of the sprayed water temperature in households is limited and largely dependent on the characteristics of the heating system as well as on the heat consumption of the system.

CONCLUSIONS

1. An effective flue gas treatment and heat recovery technology for use with small capacity pellet boilers was developed, tested, and proposed in the research, to improve the energy efficiency of the unit and the full system and to reduce particulate matter emissions. This is achieved in the fog unit, by performing heat and mass transfer processes between flue gas from the boiler and the water sprayed in the form of droplets and particulate matter.

2. The results of the fog unit system verification experiments show that the particulate matter capture efficiency of the unit can reach approximately 68 %, which is a high efficiency indicator. The main variable parameters, checked during experiments, are sprayed water flowrate, initial diameter of sprayed water droplets and droplet temperature at the inlet of the fog unit, flue gas flow and temperature before the fog unit.

3. The main indicators describing the fog unit system, obtained during the performance analysis of the system, are: capacity of the fog unit from 0.5 kW to 5.2 kW, energy efficiency from 3.2 % to 14.5 %, and particulate matter capture efficiency from 33.1 % to 67.9 %. The lowest achieved particulate matter concentration in flue gases after the FU is around 10 mg/Nm^3, which fits in the limits set by the EU Ecodesign Directive for boilers with automatic fuel feed, up to 40 mg/m^3. Experiments proved that the fog unit can provide lower PM concentration in 93 % of all cases. The only cases when particulate matter concentration exceeded 40 mg/m^3, are at increased – 30 kW boiler capacity and flowrate, whicht exceeds 250 l/h, also exceeding the optimal water flowrate. These results are applicable to operation of the unit in laboratory environment that is close to actual situation. The performance analysis of the fog unit system in artificial environment proves that the developed technology is corresponding to technology readiness level TRL 5.

4. A simulation or calculations model of the fog unit was developed within the framework of the Thesis, which describes the operation of the unit at different operation conditions. It describes heat and mass transfer processes in the condenser if particulate matter is also included in the processes. Droplet diameter, gas temperatures, water temperatures, particulate matter concentrations and water vapour saturation condition and flow partial pressure difference changes in the unit height can be determined using the model. The calculation model was validated using the comparison of experimental and calculated data at the same operational regimes of the unit. The validation was performed for data at 20 kW boiler capacity, which also describes the limits of the model at the moment. Results of the model have a high confidence level because the difference between the experimental and calculated data does not exceed 10 %.

5. The modelling results complement experimental results and offer information about processes occurring in the unit. Changes in vapour partial pressure determine whether condensation on droplets or evaporation of droplets occurs in the unit and whether processes occur in the whole unit or only in a part of it. The transition of condensation process to evaporation is topical in cases of high sprayed water temperatures, as droplets can reach dew point temperature when heated, enhancing evaporation of droplets. Determination of

parameters in the unit experimentally is complicated because the contaminated flue gases are mixed with sprayed water droplets creating a mixture of components.

6. The Box-Wilson strategy (the gradient method) is used in optimisation. Numerical experiment is performed in it. An experimental data matrix was developed and analysed for determination of the fog unit capacity, where the main parameters affecting the fog unit capacity were the flue gas flow, flue gas temperature before the fog unit (after the boiler), sprayed water amount or flowrate, water droplet diameter and sprayed water temperature at the inlet of the fog unit. The determined data limits were based on experimental results that can be equalized to the results at boiler capacities starting from 10 kW to 20 kW. The main data analysis and optimisation results show that the fog unit capacity has a linear increase trend. Practically, it is possible only until the optimal sprayed water flowrate – 150 l/h, is reached. Efficiency of the unit decreases if the sprayed water flowrate exceeds 200 l/h. Another parameter that affects the operation of the unit in practice is the flue gas flow, which cannot exceed 0.01 Nm^3/s in this specific case. The flue gas flow is affected by boiler capacity and the quality of fuel used. Additionally, the gas and droplet interaction type in the condenser must be considered.

7. The obtained results confirm that it is possible to develop an effective particulate matter capture and flue gas heat recovery equipment for heat sources in households – small capacity pellet fuel boilers. The heat recovered from flue gases can be used in hot water supply.

REFERENCES

1. "EUR-Lex – 32009L0125 – EN – EUR-Lex." [Online]. Available: https://eur-lex.europa.eu/legal-content/EN/ALL/?uri=CELEX%3A32009L0125. [Accessed: 12-Apr-2019].
2. "Noteikumi par ekodizaina prasībām ar enerģiju saistītām precēm (produktiem)." [Online]. Available: https://likumi.lv/doc.php?id=241282. [Accessed: 10-May-2019].
3. S. Fournel, B. Marcos, S. Godbout, and M. Heitz, "Predicting gaseous emissions from small-scale combustion of agricultural biomass fuels," *Bioresour. Technol.*, vol. 179, pp. 165–172, 2015.
4. J. D. Herner *et al.*, "Effect of advanced aftertreatment for PM and NOx reduction on heavy-duty diesel engine ultrafine particle emissions," *Environ. Sci. Technol.*, vol. 45, no. 6, pp. 2413–2419, 2011.
5. A. Hukkanen, T. Kaivosoja, O. Sippula, K. Nuutinen, J. Jokiniemi, and J. Tissari, "Reduction of gaseous and particulate emissions from small-scale wood combustion with a catalytic combustor," *Atmos. Environ.*, vol. 50, pp. 16–23, 2012.
6. N. Karvosenoja, Z. Klimont, A. Tohka, and M. Johansson, "Cost-effective reduction of fine primary particulate matter emissions in Finland," *Environ. Res. Lett.*, vol. 2, no. 4, p. 044002, 2007.
7. A. Messerer, V. Schmatloch, U. Pöschl, and R. Niessner, "Combined particle emission reduction and heat recovery from combustion exhaust-A novel approach for small wood-fired appliances," *Biomass and Bioenergy*, vol. 31, no. 7, pp. 512–521, 2007.
8. K. H. Kim, E. Kabir, and S. Kabir, "A review on the human health impact of airborne particulate matter," *Environ. Int.*, vol. 74, pp. 136–143, 2015.
9. E. D. Vicente and C. A. Alves, "An overview of particulate emissions from residential biomass combustion," *Atmos. Res.*, 2017.
10. Eiropas parlaments un Eiropas savienības padome, *Eiropas parlamenta un padomes direktīva 2008/50/EK par gaisa kvalitāti un tīrāku gaisu Eiropai*. 2008.
11. J. Chen *et al.*, "A review of biomass burning: Emissions and impacts on air quality, health and climate in China," *Sci. Total Environ.*, vol. 579, no. November 2016, pp. 1000–1034, 2017.
12. Clean Heat, "Residential wood burning. Environmental impact and sustainable solutions," 2016.
13. World health organization Media centre, "WHO | Ambient (outdoor) air quality and health," *WHO*, 2016.
14. C. Studies and S. Stories, "Case Studies & Success Stories," vol. I.
15. D. Broberg *et al.*, "PyCDT: A Python toolkit for modeling point defects in semiconductors and insulators," *Comput. Phys. Commun.*, vol. 226, pp. 165–179, 2018.
16. R. Wieland, K. Groth, F. Linde, and W. Mirschel, "Spatial Analysis and Modeling Tool Version 2 (SAMT2), a spatial modeling tool kit written in Python," *Ecol. Inform.*, vol. 30, pp. 1–5, 2015.
17. J. T. White, M. N. Fienen, and J. E. Doherty, "A python framework for environmental model uncertainty analysis," *Environ. Model. Softw.*, vol. 85, pp. 217–228, 2016.
18. O. Svedovs, M. Dzikevics, V. Kirsanovs, and I. Veidenbergs, "Development of New Compact Water Treatment System for Flue-Gas Condenser for Households," *Environ. Clim. Technol.*, vol. 25, no. 1, pp. 563–573, 2021.
19. O. Švedovs, M. Dzikēvičs, and V. Kirsanovs, "Methods for Determining the Performance and Efficiency Parameters of the Flue-gas Condenser Sedimentation Tank," vol. 24, no. 2, pp. 337–347, 2020.
20. V. Kostevica, "Sprauslu darbības analīze," *Bakal. darbs*, 2018.

21. ISO, “LVS EN 9096:2018,” *Starptautisks standarts*, 2018. [Online]. Available: https://www.lvs.lv/lv/products/preview/137324. [Accessed: 06-Apr-2018].
22. D. Wunsch, “Theoretical and numerical study of collision and coalescence-Statistical modeling approaches in gas-droplet turbulent flows,” 2009.
23. C. Magono and T. Nakamura, “On the Behavior with of Water a Large Droplets Water during Drop Collision,” 1959.
24. J. Monteith L. and M. Unsworth H., *Principles of Environmental Physics*, Fourth Edi. Elsevier Ltd, 2013.
25. R. Flagan C. and J. Seinfeld H., *FUNDAMENTALS OF AIR POLLUTION ENGINEERING*. Mineola New York: Dover Publications Inc., 2012.
26. N. S. Cheng, “Comparison of formulas for drag coefficient and settling velocity of spherical particles,” *Powder Technol.*, vol. 189, no. 3, pp. 395–398, 2009.
27. M. I. Shilyaev and E. M. Khromova, “Modeling of Heat and Mass Transfer and Absorption-Condensation Dust and Gas Cleaning in Jet Scrubbers,” *Intech*, vol. Chapter 7, p. 33, 2013.
28. A. O. Sæbø, R. Wighus, and R. Wighus, “Droplet sizes from deluge nozzles.”
29. F. Ahmad and R. K. Jain, “An Experimental Study of Parameters of Wet Scrubber for Environmental Benefit,” *Int. J. Innov. Res. Sci. Eng. Technol.*, vol. 5, no. 6, pp. 9675–9680, 2016.
30. D. Blumberga and I. Veidenbergs, *Tehnoloģisko gāzu attīrīšana un dzesēšana*. Rīga: Latvijas Universitāte, 1990.
31. B. A. Danzomo, M. E. Salami, S. Jibrin, and I. M. Nor, “Performance Evaluation of wet scrubber system for industrial air pollution control,” *ARPN J. Eng. Appl. Sci.*, vol. 7, no. 12, pp. 1669–1677, 2012.
32. W. Licht, *Air Pollution Control Engineering: Basic Calculations for Particulate Collection*, 2nd ed. New York: Marcel Dekker, 1988.
33. M. S. El-Morsi, “Optimization of direct contact spray coolers,” 2002.
34. S. Zheng, F. Eimann, C. Philipp, T. Fieback, and U. Gross, “Modeling of heat and mass transfer for dropwise condensation of moist air and the experimental validation,” *Int. J. Heat Mass Transf.*, vol. 120, pp. 879–894, 2018.
35. Р. И. Эстеркин, “Теплотехнические измерения при сжигании газового и жидкого топлива ... - Рахмиель Иосифович Эстеркин - Google grāmatas,” 1981. [Online]. Available: https://books.google.lv/books?id=Ll1mGwAACAAJ&dq=inauthor:%22Рахмиель+Иосифович+Эстеркин%22&hl=lv&sa=X&ved=0ahUKEwjJ4dmzqYzaAhVBqi. [Accessed: 27-Mar-2018].
36. V.-M. Tapani, “Experimental Optimization and Response Surfaces,” *Chemom. Pract. Appl.*, 2012.

Vivita Priedniece was born in 1994 in Madona. In 2016, she received a Bachelor's degree in Environmental Science and in 2018, a Master's degree in Environmental Science from Riga Technical University. The Bachelor Thesis was about biomass co-firing, but the Master Thesis was about a small droplet flue gas condenser.

In the fall of 2016, V. Priedniece started working in the Solid Biofuel Testing Laboratory of the Institute of Energy Systems and Environment of Riga Technical University. Currently V. Priedniece is a researcher and lecturer with Riga Technical University. Her research topics are related to studies of heat and mass transfer processes in flue gas, natural thermal packaging, solid biofuel testing, and combustion processes. V. Priedniece is an author and co-author of 12 scientific publications and two monographs.